

Coherent Multiple Backscattering of Waves in Random Medium beyond the Diffusion Approximation

Peter Slavov*

University of Sofia, Faculty of Physics

(Dated: November 20, 2018)

In this paper the validity of the diffusion approximation for multiple scattering of classical waves in random medium in different regimes is investigated, with emphasize to weak localization effects. Many principle topics are discussed once again. We obtain new expressions for the incoherent and coherent multiple scattering intensities for the more general case of large scattering angles and various observation points inside the medium with moving scatterers and absorption. (The results, we reached, assuming white-noise disorder for the impurities correlator, contain one-dimensional integration in its final analytical form). Also new self-consistent formulas for incoherent and coherent intensities for fixed multiplicity orders of scattering are given and their lineshapes are graphically represented. Through these formulas we clearly demonstrate that the impurities motion reduces the contribution to the intensity of the scatterings with large multiplicity orders. The total scattering intensities in 4π solid angle are calculated for the general case and compared with their diffusion approximation. For coherent intensities it is shown that a drastic deviation from the exact results occurs. It turns out that the region of angles, for which the observed lineshape of the weak localization effect tends to the incoherent background, give the main contribution to the total coherent scattered intensity. The last quantity happens to depend linearly instead of predicted quadratic dependence on the perturbation parameter, $1/k\ell$.

I. INTRODUCTION.

Anderson localization¹⁻⁷ was predicted and demonstrated as a localization of the conducting electrons. The later understanding that it is not only a quantum effect but applies as well to classical (sound or electromagnetic) waves⁸⁻¹³ stimulated a new interest in the study of propagation and multiple scattering of waves in random media¹⁴⁻²¹.

The discussion of wave localization in disordered media usually is concentrated into two characteristic regions:

(1) Region of strong localization. This is the region, where the Ioffe-Regel criterion $\ell \simeq \lambda$ is satisfied. Here λ is the *wavelength* of scattered wave and ℓ is the *elastic mean free path*. In this case the diffusion of the wave in the medium should tend to zero when the disorder becomes larger than a critical value. The transition to strong Anderson localization in both cases of quantum particles and classical waves is caused by interference effects which reduce the value of the diffusion constant until it vanishes when λ becomes of the order of ℓ . However this regime is poorly known in the interesting for us case of multiple scattering of classical waves.

(2) Region of weak localization. In this case $\ell \gg \lambda$ and the phenomenon of weak localization is identified with the effect of multiple coherent backscattering of sound or light by the disordered medium. Weak localization of light was studied extensively theoretically^{11,13-20} and experimentally²²⁻²⁴. The main result is that in a medium with a random distribution of static scatterers there is a peak in the intensity of the multiple scattered wave in a

narrow solid angle around the backward direction. This peak of light intensity is almost twice as high as the incoherent background intensity. The increase of intensity in backward direction is due to coherent interference effects.

All analytical results for the coherent backscattering intensity were obtained in diffusion approximation. Most of the authors discussing the coherent backscattering of light in random media clearly understood that this approximation is justified only at small angles, but at large angles (beyond the backscattering cone) it ceases to be valid^{11,16,19}. Therefore a careful investigation of the validity of the diffusion approximation in different regimes is needed. Similarly it is desirable to have expressions of the coherent and incoherent scattering intensities without any restriction to small angles around the backward direction. In the present paper we realize these two goals considering the explicit example of semi-infinite homogeneous medium with white noise disorder of point scatterers.

We started this work, when trying to find answers to some questions concerning the behaviour of the multiple scattering intensity in depth of the homogeneous medium:

Is there any nonzero asymptotic value of the coherent backscattering intensity at infinite depth into the homogeneous half-space? What happens with the typical lineshape of the coherent backscattering peak at various depths in the medium?

The main point in our further reasoning is the understanding that the wave localization is a phenomenon, which take place inside the scattering medium. It is clear that, if the observation point is deeper localized into the medium, the multiple scattering intensity becomes more isotropic with respect to the scattering angles. From this point of view, the investigation of the angular depen-

* petersl@phys.uni-sofia.bg

dence of both coherent and incoherent scattering intensities for 4π -geometry comes out to be an important problem. Keeping in mind these considerations, we start with obtaining the expression for the Fourier transform of the scattering propagator, based on the well known diffusion approximation. Further we find the multiple scattering intensity in this approach. The result is an increase of the incoherent intensity at infinity, to an asymptotic value, twice higher than that one on the surface at backward direction, and that the coherent intensity tends to zero at infinite depth inside of the medium. On the other hand, as we mentioned above, the diffusion approximation brings a significant error, when the angular dependence of coherent intensity is extended to 4π -geometry. We find that an additional term has been lost in the intensity expression, when the diffusion approximation has been used. In fact, this term appears, when we proceed with the exact(not approximated) ladder propagator. Using the exact propagator, we reach new results, which demonstrate that the coherent intensity at infinite depth inside of the medium tends to zero again, and the nondiffusion term turns out to be several times greater than the diffusion one. It must be noted here, that our calculations of scattered intensity were carried out, after imposing the correct image boundary conditions on the scattering propagator^{31,32}.

Further we investigate the contribution to the scattering intensity of the incoherent and coherent multiple scattering of a given multiplicity order. A comparison is made of the exact results and the diffusion approximation in this way we explicitly demonstrate that the motion of the impurities reduces the contribution of the coherent scattering with large number of scatterings. New formulas are obtained also for the total scattering intensities.

II. BASIC NOTATIONS.

A. The perturbation theory.

We shall begin with a short review of the multiple scattering of light and the commonly accepted approximations. The basic instruments, for description of propagation of waves in random media with small fluctuations, are adopted quantum field theory methods such as the Green function technique and diagram approach. The above mentioned methods applied to multiple scattering of waves and are known as *impurity-averaged perturbation theory in the small parameter* $1/kl$ and they are the ground for a quantitative theory of the multiple scattering of light. According to this theory there are two general integral equations, which one faces with – Dyson's

and Bethe-Salpeter's equations.

In what follows, we shall neglect the vector structure of the electromagnetic field (polarization effects) and we shall consider only scalar monochromatic waves. For electromagnetic waves, the randomness is caused by fluctuations of the dielectric constant, so that the disorder in the system will be described by a random part of the relative dielectric constant $\epsilon(\vec{r}) = 1 + \tilde{\epsilon}(\vec{r})$. The expression for random Green function can be directly derived from the scalar wave equation:

$$\square u(\vec{r}) - \tilde{\epsilon}(\vec{r}) \frac{\partial^2 u(\vec{r})}{c^2 \partial \tau^2} = j(\vec{r}) \quad ; \quad \vec{r} := (\vec{r}, \tau). \quad (1)$$

We shall suppose that $\tilde{\epsilon}(\vec{r})$ is a complex variable $\tilde{\epsilon}(\vec{r}) = \epsilon'(\vec{r}) + i\epsilon''$ such that its real part is a Gaussian random field $\langle \epsilon'(\vec{r}) \rangle_{ensemble} = 0$ and the imaginary part is a constant due to absorption processes $-\langle \epsilon'' \rangle_{ensemble} = \epsilon''$.

The type of disorder of the medium is given by *the correlation function of the scatterers (impurities correlator)*:

$$\psi_\epsilon(\vec{r}, \vec{r}_0) := \langle \epsilon'(\vec{r}) \epsilon'(\vec{r}_0) \rangle$$

The random scattering process is described by random Green function $G(\vec{r}, \vec{r}_0)$, which satisfies the equation:

$$\left[\square_{\vec{r}} - i\epsilon'' \frac{\partial^2}{c^2 \partial \tau^2} \right] G(\vec{r}, \vec{r}_0) - \epsilon'(\vec{r}) \frac{\partial^2 G(\vec{r}, \vec{r}_0)}{c^2 \partial \tau^2} = \delta(\vec{r} - \vec{r}_0). \quad (2)$$

The unperturbed (without the fluctuating part $\epsilon'(\vec{r})$) wave equation is:

$$\left[\square_{\vec{r}} - i\epsilon'' \frac{\partial^2}{c^2 \partial \tau^2} \right] G_0(\vec{r}, \vec{r}_0) = \delta(\vec{r} - \vec{r}_0). \quad (3)$$

The Green function technique translates the problem for obtaining the random Green function from the language of differential equations to the language of integral equations. Moreover, if we use this technique, the inclusion of source distribution becomes a trivial operation. Further we represent the random Green function as a sum of the unperturbed Green function $G_0(\vec{r}, \vec{r}_0)$ and a perturbation term. The last one can be generated, if the fluctuating term in (2) is considered as a source distribution for (3). Thus the random Green function is:

$$G(\vec{r}, \vec{r}_0) = G_0(\vec{r}, \vec{r}_0) + \int G_0(\vec{r}, \vec{r}_1) \epsilon'(\vec{r}_1) \frac{\partial^2 G(\vec{r}_1, \vec{r}_0)}{c^2 \partial \tau_1^2} d^4 \vec{r}_1 \quad (4)$$

When performing the average over the disorder $\epsilon'(\vec{r})$, we have to take into account that for a Gaussian fluctuation all odd statistical moments are zero and all even statistical moments are products of the impurities correlators:

$$\langle G(\vec{r}, \vec{r}_0) \rangle = G_0(\vec{r}, \vec{r}_0) + k_0^4 \int G_0(\vec{r}, \vec{r}_1) \psi_\epsilon(\vec{r}_1, \vec{r}_2) G_0(\vec{r}_1, \vec{r}_2) G_0(\vec{r}_2, \vec{r}_0) d^4 \vec{r}_1 d^4 \vec{r}_2 + \quad (5)$$

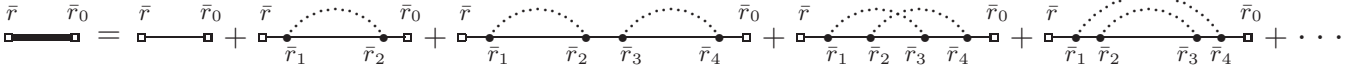


FIG. 1: Diagrammatic representation of the averaged Green function.

$$\begin{aligned}
& +k_0^8 \int G_0(\bar{r}, \bar{r}_1) \psi_\epsilon(\bar{r}_1, \bar{r}_2) G_0(\bar{r}_1, \bar{r}_2) G_0(\bar{r}_2, \bar{r}_3) \psi_\epsilon(\bar{r}_3, \bar{r}_4) G_0(\bar{r}_3, \bar{r}_4) G_0(\bar{r}_4, \bar{r}_0) d^4 \bar{r}_1 d^4 \bar{r}_2 d^4 \bar{r}_3 d^4 \bar{r}_4 + \\
& +k_0^8 \int G_0(\bar{r}, \bar{r}_1) G_0(\bar{r}_1, \bar{r}_2) \psi_\epsilon(\bar{r}_1, \bar{r}_3) G_0(\bar{r}_2, \bar{r}_3) G_0(\bar{r}_3, \bar{r}_4) \psi_\epsilon(\bar{r}_2, \bar{r}_4) G_0(\bar{r}_4, \bar{r}_0) d^4 \bar{r}_1 d^4 \bar{r}_2 d^4 \bar{r}_3 d^4 \bar{r}_4 + \\
& +k_0^8 \int G_0(\bar{r}, \bar{r}_1) \psi_\epsilon(\bar{r}_1, \bar{r}_4) G_0(\bar{r}_1, \bar{r}_2) \psi_\epsilon(\bar{r}_2, \bar{r}_3) G_0(\bar{r}_2, \bar{r}_3) G_0(\bar{r}_3, \bar{r}_4) G_0(\bar{r}_4, \bar{r}_0) d^4 \bar{r}_1 d^4 \bar{r}_2 d^4 \bar{r}_3 d^4 \bar{r}_4 + \\
& +k_0^{12} \int \dots,
\end{aligned}$$

where k_0 is the magnitude of the wave vector of the incident light. In this expansion of the averaged Green

function, each term corresponds to some order of the perturbation or equivalently to some diagram:

It is convenient to classify the different diagrams appearing on (Fig. 1) into reducible and irreducible diagrams²⁶. This way of sorting all the diagrams, enables us to rewrite the infinite sum (5) in a compact form – Dyson’s integral equation:

$$\begin{aligned}
\langle G(\bar{r}, \bar{r}_0) \rangle & = G_0(\bar{r}, \bar{r}_0) + \\
& + \int G_0(\bar{r}, \bar{r}_1) \mathcal{Q}(\bar{r}_1, \bar{r}_2) \langle G(\bar{r}_2, \bar{r}_0) \rangle d^4 \bar{r}_1 d^4 \bar{r}_2
\end{aligned} \quad (6)$$

The sum of all irreducible diagrams gives the nontrivial part of the Dyson’s equation – the kernel \mathcal{Q} of the integral operator in (6), known as mass operator. As it is seen by the definition of Dyson’s equation, the mass operator \mathcal{Q} renormalizes the free propagator G_0 .

Let us proceed now with calculation of the scattered wave intensity. Discrete random media have a very good property: to each perturbation order corresponds a given number of scatterings. To describe the wave propagation through the disordered medium we need to calculate the *4-points correlation function (or correlation function of two propagators)* defined by:

$$\Gamma(\bar{r}, \bar{r}^*; \bar{r}_0, \bar{r}_0^*) = \langle G(\bar{r}, \bar{r}_0) G^*(\bar{r}^*, \bar{r}_0^*) \rangle \quad (7)$$

Let two point-like wave sources are given in a medium. We are interested in the wave amplitudes for two arbitrary fixed points, so we intend to calculate the 4-points coherent function. Each wave, passing through a sequence of scatterings generates partial waves from various intermediate states, and they may interfere. Besides, during the scattering in the intermediate states some amplitudes, coming from one source may add to these descending to another, and these intermediate interferences are not included into the averaged Green function. The energy transfer is accounted in the correlation function of propagators and 4-points diagrams (Fig. 2). It is represented by dashed lines connecting upper and lower solid lines. Because of that the 4-point correlator is not a product of two averaged Green functions, but is the averaged product of two random Green functions. The equation between the 4-points function, the averaged Green function, and the correlation function of the scatterers (the *impurities correlator*) is called Bethe-Salpeter’s equation:

$$\Gamma(\bar{r}, \bar{r}^*; \bar{r}_0, \bar{r}_0^*) = \Gamma_0(\bar{r}, \bar{r}^*; \bar{r}_0, \bar{r}_0^*) + \int \Gamma_0(\bar{r}, \bar{r}^*; \bar{r}_1, \bar{r}_1^*) \mathcal{K}(\bar{r}_1, \bar{r}_1^*; \bar{r}_2, \bar{r}_2^*) \Gamma(\bar{r}_2, \bar{r}_2^*; \bar{r}_0, \bar{r}_0^*) d^4 \bar{r}_1 d^4 \bar{r}_1^* d^4 \bar{r}_2 d^4 \bar{r}_2^*, \quad (8)$$

where $\Gamma_0 := \langle G \rangle \langle G^* \rangle$ and the kernel \mathcal{K} of the integral

operator of the Bethe-Salpeter’s equation is the sum of

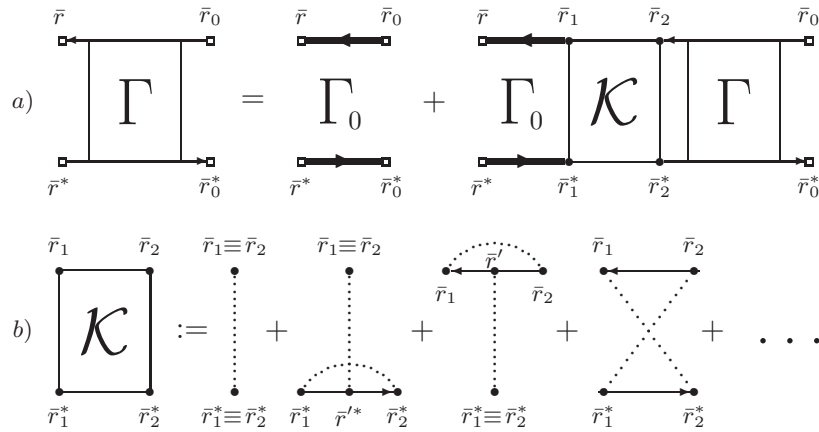


FIG. 2: a) Bethe-Salpeter's equation; b) Kernel \mathcal{K} as a sum of all irreducible diagrams.

all irreducible diagrams.

If we know the distribution of the wave sources, we may proceed to the final quantity of interest – the *correlation*

function of the scattered field :

$$\Gamma(\bar{r}, \bar{r}^*) = \langle E(\bar{r}) E^*(\bar{r}^*) \rangle = \int \Gamma(\bar{r}, \bar{r}^*; \bar{r}_0, \bar{r}_0^*) j(\bar{r}_0) j^*(\bar{r}_0^*) d^4 \bar{r}_0 d^4 \bar{r}_0^*. \quad (9)$$

Both equations (6) and (8) in the theory of wave propagation in disordered media are exact equations and their analytical solution in the general case is not known. For this reason, one natural question arises: how to do proper approximations in the mass operators \mathcal{Q} and \mathcal{K} ? Usually, the common adopted approximations do not restrict to given order of the perturbation, but to the type of irreducible diagrams taken into account.

B. The characteristic scales.

Let us briefly discuss the characteristic space-time scales, used in this study. The first scale is set by the *total mean free path* and the mean time between two scatterings. The variables, which vary in intervals of the order of this scale will be denoted by capital letters. The impurities correlator decreases rapidly with the distance $|\bar{r}_1 - \bar{r}_2|$, so it determines another characteristic scale, in which particle radius, time for passing the particle size and life-time of the excitations are included. The variables, which change inside that scale, will be denoted by small letters. When we calculate quantities of interest, we face with integration over distances from $-\infty$ to $+\infty$. In this case some additional approximations may be done

under the integral. Nevertheless, we should treat the sign ∞ not as an absolute symbol, but as a quantity, attached to one of the above mentioned scales. Such a case is realized when we assume the Fraunhofer approximation to be valid under the integral.

Note that the large scale imposes a restriction to the medium size. For example, a scattering slab must not be smaller than the *total mean free path*¹⁹. Moreover, the incident wave packet must not have a coherent length, smaller than the total mean free path.

In what follows, we introduce large scale coordinates

$$\vec{R} := \frac{\vec{r} + \vec{r}^*}{2} \quad T := \frac{\tau + \tau^*}{2}$$

and relative coordinates

$$\vec{r} := \vec{r} - \vec{r}^* \quad t := \tau - \tau^* .$$

Finally, we would like to draw attention to another important question, related to the two characteristic space-time scales. In general, the impurities correlator depends dominantly on the spatial separation $|\vec{r}_1 - \vec{r}_2|$. When this separation is comparable to the characteristic length of the large scale, the impurities correlator tends to zero. In contrast, in the case of small separations $|\vec{r}_1 - \vec{r}_2|$, close

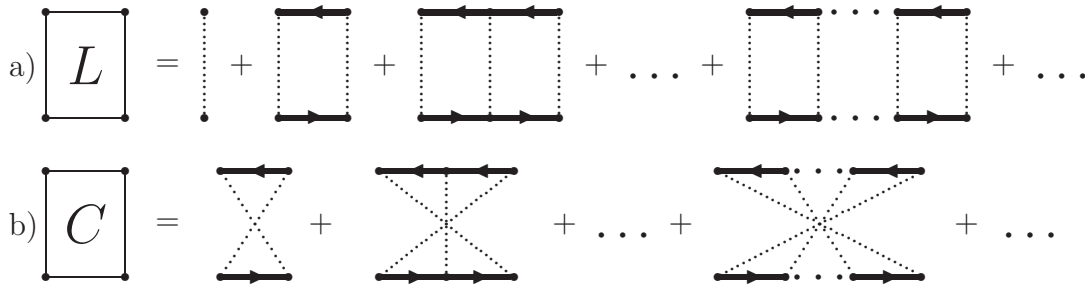


FIG. 3: (a) Ladder diagrams. (b) Maximally crossed diagrams.

to the characteristic length of scale of microstructures, the correlators ψ_ϵ give a considerable contribution to Γ in different perturbation orders. However, only ladder diagrams expansion of Γ (Fig. 3(a)) contains the impu-

rities correlators with such small magnitudes of $|\vec{r}_1 - \vec{r}_2|$. That's why, the principal contribution to the 4-points correlation function is given by the ladder diagrams.

On the other hand, if the disordered medium has a *time-reversal symmetry*, the maximally-crossed diagrams (Fig. 3(b)) may be converted to ladder type diagrams by a time-reversal operation^{11,19,33}. Therefore, for a time-reversal invariant medium, the maximally-crossed diagrams give a significant correction (in order $1/k\ell$) to Γ . These diagrams describe the experimentally observed effect of coherent backscattering of light. It must be pointed out here, that this effect of intensity amplification at backward direction is due only to the time-reversal symmetry of the scattering medium, but not to the statistics of the impurities¹¹. The effect of coherent backscattering may be described physically by the constructive interference of a given multiple scattering path with itself but time-reversed. If the medium does not have a time-reversal symmetry, the maximally-crossed diagrams can not be represented as time-reversed ladder diagrams. That's why, in the case of broken time-reversal symmetry, their contribution to Γ becomes negligible.

C. Coherent potential approximation.

Let us now determine the averaged Green function. This requires to fix the approximation for the integral operator \mathcal{Q} in the Dyson's equation. In addition we suggest that the average over the disorder $\tilde{\epsilon}$ restores translational symmetry, so our quantities of interest will depend on the spatial separation $|\vec{r} - \vec{r}'|$. Commonly accepted approach is the simplest one, called *coherent potential approximation*¹⁹:

$$\begin{aligned} G(\vec{r}_1 - \vec{r}_2, t_1 - t_2) &:= G_0(\vec{r}_1, \vec{r}_2) \Phi(\vec{r}_1 - \vec{r}_2; \tau_1 - \tau_2) \\ \Phi(\vec{r}_1 - \vec{r}_2; \tau_1 - \tau_2) &:= k_0^4 \psi_\epsilon(\vec{r}_1, \vec{r}_2; t_1, t_2), \end{aligned} \quad (10)$$

where Φ is the impurities correlator multiplied by k_0^4 . This first order approximation for \mathcal{Q} has the following diagrammatic representation:

$$\mathcal{Q} \approx \begin{array}{c} \text{---} \text{---} \text{---} \\ \bullet \text{---} \text{---} \text{---} \bullet \\ \vec{r}_1 \qquad \vec{r}_2 \end{array}$$

Such assumption for \mathcal{Q} leads to the following Fourier transform of Dyson's equation :

$$\langle G(\vec{k}, k_0) \rangle^{-1} = G_0(\vec{k}, k_0)^{-1} - \mathcal{Q}(\vec{k}, k_0), \quad (11)$$

where

$$\mathcal{Q}(\vec{k}, k_0) = (2\pi)^{-4} \int G_0(\vec{k}', k'_0) \Phi(\vec{k} - \vec{k}', k_0 - k'_0) d^3k' dk'_0. \quad (12)$$

D. White-noise approximation.

The impurities correlator is determined by the size and motion of the scatterers. Furthermore, it may depend on the interactions between the scattering particles. The simplest assumption for the impurities correlator is a the *white-noise approximation*. It means:

- 1/ low density of the impurities;
- 2/ uncorrelated disorder – no interactions between the scattering particles;
- 3/ point-like scatterers;
- 4/ nonrelativistic motion of the impurities;
- 5/ structureless scattering particles – not any internal excitations;
- 6/ absence of any incoherent quantum effects, like Compton effect, etc.

For low densities and for noninteracting particles the correlation function of scatterers is proportional to the density of scattering particles and has width, approximately equal to the particle radius²⁰. The essence of the white-noise model consists in the following: for scattering particles of size, a , much smaller than the wavelength of light ($a \ll \lambda$), the Fourier-transformed correlator $\Phi(\vec{q}, t)$ will be almost independent of the scattering transfer vector \vec{q} , and hence the scattering will be isotropic. Besides, during the field transport from one point to another within the medium, all transfers of the intermediate wave vectors conserve their magnitudes $|\vec{k}_j| = k_0$.

To proceed further, we first must define the *total mean free path* ℓ , which plays an important role as a basic scale unit. It is given by:

$$\frac{1}{\ell} := \frac{1}{\ell_i} + \frac{1}{\ell_e}, \quad \ell_i := \frac{1}{k_0 \epsilon''}, \quad \ell_e(\omega) := \frac{4\pi c^4}{n \epsilon_*^2 \omega^4}, \quad (13)$$

where ℓ_i is the *inelastic mean free path*, due to the absorption processes, ℓ_e is the *elastic mean free path*, n is density of impurities and ϵ_* is polarizability of scatterers.

For stationary white noise model the correlator ψ_ϵ is a delta function in spatial variables, normalized to $4\pi/\ell_e k_0^4$ ¹⁹. Therefore the Fourier transform of Φ becomes $4\pi/\ell_e \delta(k_0 - k'_0)$ and one can obtain for (12) the result ik_0/ℓ_e . Replacing it in (11) and using the Fourier transform of unperturbed Green function:

$$G_0^{+/-}(\vec{k}, k_0) = \frac{1}{k^2 - k_0^2 \mp ik_0/\ell_i},$$

we obtain the averaged Green function:

$$\langle G^{+/-}(\vec{k}, k_0) \rangle = \frac{1}{k^2 - k_0^2 \mp ik_0/\ell}. \quad (14)$$

Here the subscripts ”+” and ”-” denote advanced and retarded propagators.

Let us now consider the time-dependent white-noise model. In this case the scattered intensity is related to the Fourier transform of the correlation function¹⁷:

$$\Phi(\vec{q}, t) = \frac{4\pi}{\ell_e} \exp(-a(t) \vec{q}^2) \quad (15)$$

where \vec{q} is the transfer wave-vector and $a(t)$ describes the character of the impurities motions. The effect of

particle dynamics on the multiple scattering of light has been discussed in¹¹ and¹⁷ for two special cases:

(1) the scatterers have a Maxwell-Boltzmann velocity distribution; and

(2) the scatterers are themselves diffusing in the medium with a given diffusion constant.

In our further investigations we shall not specify the form of the correlator $\Phi(\vec{q}, t)$. In general, we assume nonrelativistic motions of scatterers $\sqrt{\langle v^2 \rangle}/c \ll 1$. Then the frequency change during scattering is negligible $\Delta\omega/\omega_0 \ll 1$ and we can consider the propagation of an almost-monochromatic wave with frequency close to the frequency of the incident light ω_0 . According to this assumption Φ will not depend in an important way on $a(t)$. Then the Fourier transform of \mathcal{Q} , expression(12), coincides with the stationary one, after the formal replacement $k_0 \rightarrow \omega/c$. Therefore the averaged Green function in (k, ω) -representation gets the same form as (14). The propagation of a scalar wave in an infinite medium is described by the retarded Green function:

$$D(\vec{r} - \vec{r}', \omega) = \frac{\exp\left[i\frac{\omega}{c}|\vec{r} - \vec{r}'| - \frac{1}{2\ell(\omega)}|\vec{r} - \vec{r}'|\right]}{4\pi|\vec{r} - \vec{r}'|} \quad (16)$$

where $D := \langle G^- \rangle$.

III. THE SUM OF LADDER DIAGRAMS.

In the weak scattering limit $\lambda \ll \ell$ the leading approximation to the 4-points correlation function Γ is given by the sum of ladder diagrams, represented in (Fig. 3(a)).

The ladder propagator describes the incoherent multiple scattering of light through the medium, i.e. the ordinary diffusion in the medium. To obtain the sum of ladder diagrams, we must include only the ladder term in the expansion of \mathcal{K} . The Bethe-Salpeter's equation then reduces to an integral equation for the ladder propagator. Further we will use large scale and relative coordinates, introduced in section II B . The propagator L is most easily calculated in (\vec{k}, ω) -space. The Fourier transform of the sum of ladder diagrams then satisfies the integral equation:

$$L(\vec{K}, \Omega; k_0 \vec{S}_1, \omega_1; k_0 \vec{S}_2, \omega_2) = \Phi(k_0(\vec{S}_1 - \vec{S}_2), \omega_1 - \omega_2) + \quad (17)$$

$$+ (2\pi)^{-4} \int \Phi(k_0 \vec{S}_1 - \vec{k}, \omega_1 - \omega) D\left(\vec{k} + \frac{\vec{K}}{2}, \omega + \frac{\Omega}{2}\right) D^*\left(\vec{k} - \frac{\vec{K}}{2}, \omega - \frac{\Omega}{2}\right) L(\vec{K}, \Omega; k_0 \vec{S}_1, \omega; k_0 \vec{S}_2, \omega_2) d\vec{k} d\omega,$$

where Ω is the frequency change during scattering, and

\vec{S}_1, \vec{S}_2 are unit vectors.

In the weak scattering regime the Fraunhofer approximation is allowed:

$$D(\vec{R} + \frac{\vec{r}}{2}, \omega + \frac{\Omega}{2}) \approx \exp\left(ik_0\vec{S}_R \cdot \frac{\vec{r}}{2}\right) D(\vec{R}, \omega + \frac{\Omega}{2}) ; \vec{S}_R := \frac{\vec{R}}{|\vec{R}|} \quad (18)$$

According to this approximation the product of retarded and advanced Green functions becomes:

$$D\left(\vec{k} + \frac{\vec{K}}{2}, \omega + \frac{\Omega}{2}\right) D^*\left(\vec{k} - \frac{\vec{K}}{2}, \omega - \frac{\Omega}{2}\right) = (2\pi)^3 \int \delta(\vec{k} - k_0\vec{S}_R) e^{-i\vec{K} \cdot \vec{R}} D\left(\vec{R}, \omega + \frac{\Omega}{2}\right) D^*\left(\vec{R}, \omega - \frac{\Omega}{2}\right) d^3\vec{R} \quad (19)$$

Replacing (19) in the integral equation (17), we get:

$$L(\vec{K}, \Omega; k_0\vec{S}_1, \omega_1; k_0\vec{S}_2, \omega_2) = \Phi\left(k_0(\vec{S}_1 - \vec{S}_2), \omega_1 - \omega_2\right) + (2\pi)^{-1} \int \Phi\left(k_0(\vec{S}_1 - \vec{S}_R), \omega_1 - \omega\right) e^{-i\vec{K} \cdot \vec{R}} Q(\vec{R}, \Omega, \omega) L(\vec{K}, \Omega; k_0\vec{S}_1, \omega; k_0\vec{S}_2, \omega_2) d^3\vec{R} d\omega, \quad (20)$$

where

$$Q(\vec{R}, \Omega, \omega) := D\left(\vec{R}, \omega + \frac{\Omega}{2}\right) D^*\left(\vec{R}, \omega - \frac{\Omega}{2}\right) = \frac{\exp\left[i\frac{\Omega}{c} - \frac{1}{2\ell(\omega + \frac{\Omega}{2})} - \frac{1}{2\ell(\omega - \frac{\Omega}{2})}\right] R}{(4\pi R)^2} \quad (21)$$

For small frequency change on scattering $\Omega \ll \omega$ expression (13) for ℓ becomes:

$$\ell^{-1}\left(\omega \pm \frac{\Omega}{2}\right) \approx \ell_i^{-1} + \ell_e^{-1}(\omega) \left(1 \pm 2\frac{\Omega}{\omega}\right) \quad (22)$$

and

$$Q(R, \Omega, \omega) \approx (4\pi R)^{-2} \exp\left[\left(i\frac{\Omega}{c} - \frac{1}{\ell(\omega)}\right) R\right] \quad (23)$$

In the stationary case the correlator Φ turns out to be

$$L_{n+1}(\vec{K}, \Omega; k_0\vec{S}_1, k_0\vec{S}_2; t) = \int \Phi\left(k_0(\vec{S}_1 - \vec{S}_R), t\right) e^{-i\vec{K} \cdot \vec{R}} Q(\vec{R}, \Omega) L_n(\vec{K}, \Omega; k_0\vec{S}_R, k_0\vec{S}_2; t) d^3\vec{R} \quad (24)$$

Let us assume that *s-wave approximation* is valid, i.e. the *bare diffusion propagator* describes propagation of a spherical wave. It means that $L_n(\vec{K}, \Omega; k_0\vec{S}_1, k_0\vec{S}_2; t)$ is independent on the directions:

$$L_n(\vec{K}, \Omega; k_0\vec{S}_1, k_0\vec{S}_2; t) \approx L_n(\vec{K}, \Omega, t), \quad (25)$$

a δ -function with respect to ω , and in the nonstationary case the last one is almost δ -function. This circumstance afford us to take $Q(\vec{R}, \Omega, \omega) = Q(\vec{R}, \Omega)$ in the integrand of (20). So without any loss of generality we get $L(\vec{K}, \Omega; k_0\vec{S}_1, \omega_1; k_0\vec{S}_2, \omega_2) = L(\vec{K}, \Omega; k_0\vec{S}_1, k_0\vec{S}_2; \omega_1 - \omega_2)$ and perform the Fourier transformation with respect to ω ($\omega \rightarrow t$) in (20). Taking into account that L satisfies equation (20), we derive the relation between the $(n+1)^{\text{th}}$ and n^{th} generic terms of the sum L :

where

$$L_n(\vec{K}, \Omega, t) := (4\pi)^{-2} \int L_n(\vec{K}, \Omega; k_0\vec{S}_1, k_0\vec{S}_2; t) d^3\vec{S}_1 d^3\vec{S}_2. \quad (26)$$

Note that **for the stationary case in white-noise model eq.(25) becomes an exact equation** as far as the Fraunhofer approximation has already been assumed. For the nonstationary case *the s-wave approximation* follows from the Fraunhofer approximation and from **the quite weak angular dependence of the impurities**

correlator. In some papers^{11,17} it was related to the diffusion approximation, but in our opinion it follows from **the weak scattering approximation**, which permits doing the Fraunhofer approximation. As we will see below **the weak scattering does not require the diffusion approximation.**

Let us define the angular averaged correlator¹¹:

$$\gamma f(t) := \int \Phi(k_0(\vec{S}_1 - \vec{S}_2), t) \frac{d^3 \vec{S}_2}{4\pi}, \quad \gamma := \frac{4\pi}{\ell_e}. \quad (27)$$

Then each term fulfills the relation:

$$L_{n+1}(\vec{K}, \Omega, t) = \gamma f(t) Q(\vec{K}, \Omega) L_n(\vec{K}, \Omega, t), \quad n = 1, 2, \dots \quad (28)$$

From this point on the single-scattering term will be explicitly separated:

$$L = L_1 + \tilde{L}, \quad L_1(\vec{K}, \Omega, t) := \gamma f(t)$$

$$\tilde{L}(\vec{K}, \Omega; t) = \gamma^2 f^2(t) Q(\vec{K}, \Omega) + \gamma f(t) Q(\vec{K}, \Omega) \tilde{L}(\vec{K}, \Omega; t) \quad (29)$$

where the function $Q(K, \Omega)$ has the following form:

$$Q(K, \Omega) = \frac{1}{8\pi K} [\arctg(K\ell + \frac{\Omega}{c}\ell) + \arctg(K\ell - \frac{\Omega}{c}\ell)] + \frac{i}{16\pi K} \{ \ln[1 + (K\ell + \frac{\Omega}{c}\ell)^2] - \ln[1 + (K\ell - \frac{\Omega}{c}\ell)^2] \} \quad (30)$$

Furthermore, the sum of ladder diagrams may be written as a geometric series in the variable $\gamma f(t) Q(K, \Omega)$:

$$\tilde{L}(K, \Omega; t) = \sum_{n=1}^{\infty} L_{n+1}(K, \Omega, t) \quad (31)$$

$$L_{n+1}(K, \Omega, t) := \gamma f(t) (\gamma f(t) Q(K, \Omega))^n.$$

For nonrelativistic motions of scatterers, the frequency change on scattering is negligible, i.e. $\Omega/\omega_0 \ll 1$, so we can replace $\Omega = 0$:

$$\gamma Q(K) := \gamma Q(K, 0) = \frac{\ell}{\ell_e} \frac{\arctg(K\ell)}{K\ell} \quad (32)$$

and the $(n+1)$ th ladder term gets the form:

$$L_{n+1}(K, t) = \frac{4\pi}{\ell} g(t) \left(g(t) \frac{\arctg(K\ell)}{K\ell} \right)^n, \quad (33)$$

$$g(t) := \frac{\ell}{\ell_e} f(t) = \frac{f(t)}{1+\mu} \leq 1.$$

On taking the Fourier transformation with respect to \vec{K} , we obtain:

$$L_{n+1}(R, t) = \frac{g^{n+1}(t)}{i\pi R \ell^3} \int_{-\infty}^{+\infty} e^{i\frac{R}{\ell} p} \left(\frac{\arctg p}{p} \right)^n p dp \quad (34)$$

Evaluation of the integral (34) in the complex plane is described in Appendix (96). The result is :

$$L_{n+1}(R, t) = \frac{g^{n+1}(t)}{\pi R \ell^3} \int_1^{\infty} \frac{\exp(-R \frac{u}{\ell})}{(2u)^{n-1}} \left(\ln^2 \frac{u+1}{u-1} + \pi^2 \right)^{\frac{n}{2}} \sin \left(n \arctg \frac{\pi}{\ln \frac{u+1}{u-1}} \right) du \quad (35)$$

This is the final analytical form for $L_{n+1}(R, t)$, we can reach in the case of s -wave approximation. The expressions for $L_2(R, t), \dots, L_7(R, t)$ are given in Appendix (97).

The geometric series (31) are convergent for all K , since $0 \leq g(t) \frac{\arctg(K\ell)}{K\ell} < 1$. Then the sum of ladder diagrams (without single-scattering term) in wave-vector space is:

$$\tilde{L}(K; t) = \frac{4\pi}{\ell} \frac{g(t) \frac{\arctg(K\ell)}{K\ell}}{g^{-1}(t) - \frac{\arctg(K\ell)}{K\ell}}, \quad (36)$$

and the ladder propagator in coordinate space is given by:

$$\tilde{L}(\vec{R}; t) = \frac{g(t)}{2\pi^2 \ell} \int \frac{e^{i\vec{K} \cdot \vec{R}} \frac{\arctg(K\ell)}{K\ell}}{g^{-1}(t) - \frac{\arctg(K\ell)}{K\ell}} d^3 \vec{K}. \quad (37)$$

Let us now define *effective diffusion length* by the tran-

scendent equation²⁵:

$$\frac{1}{2\chi} \ln \frac{1+\chi}{1-\chi} = g^{-1}(t) \quad g(t) \leq 1 \quad (38)$$

The *effective diffusion length* (in units of total mean free path ℓ) is defined as the reciprocal value of the root of equation (38) – χ^{-1} . The quantity $\chi^{-1} + 1$ represents the *effective order of scattering*. We have to point out here that the *effective diffusion length* does not impose any rigid restriction to the long diffusion paths, i.e. there exist diffusion paths greater than χ^{-1} even in the case of very large effective diffusion lengths. The magnitude of χ^{-1} influences only the speed of convergence of the infinite sum \tilde{L} .

In fact, the root of transcendent equation (38) gives the two poles at $\pm i\chi$ in the integrand of (37). Evaluation of integral (37) is carried out in the complex plane (see Appendix). The final result for the sum of ladder diagrams (without single-scattering term) is:

$$\tilde{L}(\vec{R}; t) = \frac{1}{R\ell^3} \left[A(\chi(t)) \exp\left(-\frac{R}{\ell}\chi(t)\right) + \int_1^\infty \frac{\exp(-R\frac{u}{\ell}) du}{\left(g^{-1}(t) - \frac{1}{2u} \ln \frac{u+1}{u-1}\right)^2 + \frac{\pi^2}{4u^2}} \right], \quad A(\chi(t)) := \frac{2\chi^2(t)}{(1-\chi^2(t))^{-1} - g^{-1}(t)} \quad (39)$$

It is convenient to define an integral operator $\mathcal{F}(g(t))$ by:

$$\mathcal{F}(g(t)) [H(u, \dots)] := A(\chi(t)) H(\chi(t), \dots) + \int_1^\infty \frac{H(u, \dots) du}{\left(g^{-1}(t) - \frac{1}{2u} \ln \frac{u+1}{u-1}\right)^2 + \frac{\pi^2}{4u^2}} \quad (40)$$

where $H(u, \dots)$ is an uniformly continuous function. Then:

$$\tilde{L}(|\vec{R}_1 - \vec{R}_2|; t) = \mathcal{F}(g(t)) \left[\frac{\exp\left(-\frac{|\vec{R}_1 - \vec{R}_2|}{\ell} u\right)}{|\vec{R}_1 - \vec{R}_2| \ell^3} \right] \quad (41)$$

The first term in (39) corresponds to the familiar diffusion propagator²⁵ and **the second term becomes significant when the contributions of higher scattering orders (or equivalently long diffusion paths) to \tilde{L} are negligible.**

The N^{th} -order expansion of (38) is:

$$\frac{1}{2\chi} \ln \frac{1+\chi}{1-\chi} \approx \sum_{n=0}^N \frac{\chi^{2n}}{2n+1}, \quad (42)$$

$$\frac{1}{2\chi^2} \left(\frac{1}{1-\chi^2} - \frac{1}{2\chi} \ln \frac{1+\chi}{1-\chi} \right) \approx \sum_{n=1}^N \frac{n\chi^{2n-2}}{2n+1}$$

In the limits of large effective diffusion lengths $\chi \ll 1$, the first order approximation ($N=1$) is acceptable:

$$\begin{aligned} g^{-1}(t) \approx 1 + \frac{1}{3}\chi^2 &\Rightarrow \chi^2 \approx \chi_1^2 := 3g^{-1}(t) - 3; \quad (43) \\ &\Rightarrow \frac{1}{2\chi_1^2} \left(\frac{1}{1-\chi_1^2} - g^{-1}(t) \right) \approx \frac{1}{3} \end{aligned}$$

For $N=1$ in the stationary case ($f(t)=1$), without absorption ($g(t)=f(t)$), the exact result for the sum of ladder diagrams follows:

$$\tilde{L}(R) = \mathcal{F}(1) \left[\frac{\exp(-R\frac{u}{\ell})}{R\ell^3} \right] = \frac{1}{R\ell^3} \left[3 + \int_1^\infty \frac{\exp(-R\frac{u}{\ell}) du}{\left(1 - \frac{1}{2u} \ln \frac{u+1}{u-1}\right)^2 + \frac{\pi^2}{4u^2}} \right] \quad (44)$$

IV. BOUNDARY CONDITIONS FOR A SEMI-INFINITE MEDIUM.

Up to now, we have obtained the sum of ladder diagrams (39) in the case of an infinite scattering medium. However, our aim is to study the light reflected by a semi-infinite scattering medium occupying the half-space $Z > 0$. In order to solve this task we must impose proper boundary conditions on the propagator \tilde{L} . It satisfies an integral equation, which has the following diagrammatic form:

$$\tilde{L} = L_2 + \tilde{L}$$

The usual approximation made is that the term L_2 is too small in the infinite sum \tilde{L} . By this way, the upper integral equation may be reduced to the Milne's integral

equation:

$$\tilde{L} = \tilde{L}$$

When the *effective diffusion length* χ^{-1} approaches infinity, the sum $\tilde{L}(K)$ is a geometric series with $Q(K) \lesssim 1$, so that the contribution of $L_2(K)$ to the scattering propagator is truly small. This situation corresponds to the case of stationary macro scatterer, without absorption losses in it. However, when the *effective diffusion length* decreases significantly and becomes close to 1 (*effective diffusion length* \approx *elastic mean free path*), then in accordance with the strong convergence of \tilde{L} , the contributions of lower scattering orders (in particular L_2) become important. That's why in this case, reducing the integral equation for \tilde{L} to the Milne's one brings a small error.

The integral Milne's equation has the advantage to be solved exactly for point-like scatterers, by mean of the Wiener-Hopf method^{25,31}. It can be shown that very far from the surface of the medium ($Z \gg \ell$) \tilde{L} obeys a diffusion equation^{19,25,31} with the boundary condition $\tilde{L}(-Z_{as}) = 0$. It means that the diffusion propagator (the asymptotic form of \tilde{L} when $R \rightarrow \infty$) vanishes on a trapping plane, located at an extrapolation distance $-Z_{as}$. The computation of Z_{as} was carried out with high precision³¹:

$$M_{as} := \frac{Z_{as}}{\ell} = 0.710\,446.$$

It should be noted, that the asymptotic boundary condition proposed above gives a correct solution of the Milne's equation only in the diffusion approximation. However, when we are concerned with the coherent intensity for large scattering angles, we should correct the ex-

trapolation distance Z_{as} ¹⁶. The exact solution of Milne's integral equation, beyond the diffusion approximation, has been obtained by Mark³². Imposing the boundary condition for a semi-infinite medium on it, we obtain the correct location of the trapping plane as a root of an algebraic equation (see appendix 103). In our further calculations of scattered intensity we shall adopt the exact Milne's number:

$$M := \frac{Z_0}{\ell} = 0.689\,710,$$

which gives the effective boundary for the case of infinite *effective diffusion length*.

As the explicit form of the ladder propagator for an infinite homogeneous medium has already been found, we could obtain \tilde{L} for a half-space, using the exact boundary condition and the well known method of images:

$$\tilde{L}(\vec{R}_1, \vec{R}_2; t) := \int \tilde{L}(\vec{K}; t) \left[e^{i\vec{K} \cdot (\vec{R}_1 - \vec{R}_2)} - e^{i\vec{K} \cdot (\vec{R}_1 - \vec{R}_2^*)} \right] \frac{d^3\vec{K}}{(2\pi)^3} = \tilde{L}(\vec{R}_1 - \vec{R}_2; t) - \tilde{L}(\vec{R}_1 - \vec{R}_2^*; t), \quad (45)$$

so that

$$\tilde{L}(\vec{R}_1, \vec{R}_2; t) = 0 \quad \text{as} \quad \vec{R}_2 = \vec{R}_2^*,$$

where the images are located at

$$\vec{R}_2 := (X_2, Y_2, Z_2), \quad \vec{R}_2^* := (X_2, Y_2, Z_2^*), \quad Z_2^* := -Z_2 - 2Z_0.$$

In conclusion it may be stressed that the main differences between the diffusion approximation and our approach consist in:

1/The way, in which the propagator $\tilde{L}(\vec{R}_1 - \vec{R}_2; t)$ is defined eq.(39).

2/The value of the parameter M .

V. INCOHERENT MULTIPLE SCATTERING INTENSITY.

We have obtained the sum of ladder diagrams (39), which characterizes the scattering medium. The distribution of the wave sources is known. Then we may proceed to the calculation of the part of the time-dependent correlation function, describing the multiple incoherent scattering. It is defined by:

$$\begin{aligned} \Gamma_{\tilde{L}}(\vec{R}, \vec{r}; T, t) := & \int D\left(\vec{R} - \vec{R}_1 + \frac{\vec{r} - \vec{r}_1}{2}, T - T_1 + \frac{t - t_1}{2}\right) D^*\left(\vec{R} - \vec{R}_1 - \frac{\vec{r} - \vec{r}_1}{2}, T - T_1 - \frac{t - t_1}{2}\right) \times \\ & \times \tilde{L}\left(\vec{R}_1, \vec{R}_2, \vec{r}_1, \vec{r}_2; T_1, T_2, t_1, t_2\right) E\left(\vec{R}_2 + \frac{\vec{r}_2}{2}, T_2 + \frac{t_2}{2}\right) E^*\left(\vec{R}_2 - \frac{\vec{r}_2}{2}, T_2 - \frac{t_2}{2}\right) d^3\vec{R}_1 d^3\vec{R}_2 d^3\vec{r}_1 d^3\vec{r}_2 dT_1 dT_2 dt_1 dt_2 \end{aligned} \quad (46)$$

Since the medium is invariant under translations of T we have:

$$\tilde{L}(\vec{R}_1, \vec{R}_2, \vec{r}_1, \vec{r}_2; T_1, T_2, t_1, t_2) = \tilde{L}(\vec{R}_1, \vec{R}_2, \vec{r}_1, \vec{r}_2; T_1 - T_2, t_1, t_2) \quad (47)$$

If we assume that the fields are monochromatic waves $E(\vec{R}, t) := E(\vec{R})e^{-i\omega_0 t}$, after Fourier transformation of the functions under the integral (46) with respect to the time variables, we obtain:

$$\Gamma_{\tilde{L}}(\vec{R}, \vec{r}; T, t) = \Gamma_{\tilde{L}}(\vec{R}, \vec{r}; t) = e^{-i\omega_0 t} \int e^{i(\omega + \omega_0)t} D\left(\vec{R} - \vec{R}_1 + \frac{\vec{r} - \vec{r}_1}{2}, \omega\right) D^*\left(\vec{R} - \vec{R}_1 - \frac{\vec{r} - \vec{r}_1}{2}, \omega\right) \times \quad (48)$$

$$\times \tilde{L}(\vec{R}_1, \vec{R}_2, \vec{r}_1, \vec{r}_2; \omega, -\omega_0) E\left(\vec{R}_2 + \frac{\vec{r}_2}{2}\right) E^*\left(\vec{R}_2 - \frac{\vec{r}_2}{2}\right) d\frac{\omega+\omega_0}{2\pi} d^3\vec{R}_1 d^3\vec{R}_2 d^3\vec{r}_1 d^3\vec{r}_2$$

The integration over $d^3\vec{r}_1$, $d^3\vec{r}_2$ and $d\frac{\omega+\omega_0}{2\pi}$ gives the Fourier transform $\tilde{L}(\vec{R}_1, \vec{R}_2, k_0\vec{S}_{RR_1}, k_0\vec{S}_{R_2}; t)$, so the field correlation function becomes:

$$\Gamma_{\tilde{L}}(\vec{R}, \vec{r}; t) = \frac{e^{-i\omega_0 t}}{16\pi^2} \int \exp(ik_0\vec{S}_{RR_1}\vec{r}) \frac{\exp\left(\frac{-|\vec{R}-\vec{R}_1|}{\ell}\right)}{(\vec{R}-\vec{R}_1)^2} \tilde{L}(\vec{R}_1, \vec{R}_2, k_0\vec{S}_{RR_1}, k_0\vec{S}_{R_2}; t) |E(\vec{R}_2)|^2 d^3\vec{R}_1 d^3\vec{R}_2 \quad (49)$$

Taking into account that in s -wave approximation $\tilde{L}(\vec{R}_1, \vec{R}_2, k_0\vec{S}_{RR_1}, k_0\vec{S}_{R_2}; t) = \tilde{L}(\vec{R}_1, \vec{R}_2; t)$, after Fourier transformation we get:

$$\Gamma_{\tilde{L}}(\vec{R}, \vec{k}; t) := \int e^{-i\vec{k}\cdot\vec{r}} \Gamma_{\tilde{L}}(\vec{R}, \vec{r}; t) d^3\vec{r} = \frac{\pi e^{-i\omega_0 t}}{2} \int \delta(\vec{k} - k_0\vec{S}_{RR_1}) \frac{\exp\left(\frac{-|\vec{R}-\vec{R}_1|}{\ell}\right)}{(\vec{R}-\vec{R}_1)^2} \tilde{L}(\vec{R}_1, \vec{R}_2; t) |E(\vec{R}_2)|^2 d^3\vec{R}_1 d^3\vec{R}_2 \quad (50)$$

The correlation function of the wave field $\Gamma_{\tilde{L}}(\vec{R}, \vec{k}; t)$ describes the intensity of the incoherent multiple scattering scalar wave, which has a wave vector \vec{k} in the point \vec{R} . The intensity in this point, for a given direction \vec{S} , can be obtained after integrating over the wave vector magnitude.

$$J^{\tilde{L}}(\vec{R}, \vec{S}; t) := 2 \int_0^\infty k^2 \Gamma_{\tilde{L}}(\vec{R}, \vec{k}; t) dk \quad (51)$$

In the case of semi-infinite medium we have a cylindrical symmetry. Z -axis is chosen to be normal to the surface

and is orientated inside the medium. The other two axes can be orientated in such way, that:

$$\vec{S} := \frac{\vec{k}}{k} := (\sin\alpha, 0, \cos\alpha) \quad \alpha := \angle(\vec{OZ}, \vec{S}) \quad (52)$$

According to the translation symmetry with respect to X and Y directions, without any limitation of generality we may choose $\vec{R} := (0, 0, Z)$. Then

$$\delta(k\vec{S} - k_0\vec{S}_{RR_1}) = \begin{cases} \frac{(Z-Z_1)^2}{k_0^2 \cos^3\alpha} \delta(k-k_0) \delta(X_1 + \text{tg}\alpha(Z-Z_1)) \delta(Y_1) \theta\left(\frac{Z-Z_1}{\cos\alpha}\right) & ; \alpha \neq \pi/2 \\ \frac{X_1^2}{k_0^2} \delta(k-k_0) \delta(Y_1) \delta(Z-Z_1) \theta(-X_1) & ; \alpha = \pi/2 \end{cases} \quad (53)$$

and

$$J^{\tilde{L}}(Z, \alpha, t) = \frac{\pi e^{-i\omega_0 t}}{|\cos\alpha|} \int \theta\left(\frac{Z-Z_1}{\cos\alpha}\right) \exp\left(\frac{Z_1-Z}{\ell \cos\alpha}\right) |E(\vec{\rho}, Z_2)|^2 \tilde{L}(-\text{tg}\alpha(Z-Z_1), 0, Z_1; \vec{\rho}, Z_2; t) \vec{\rho} dZ_2 dZ_1, \quad (54)$$

where $\theta(X)$ is the Heaviside step function and $\vec{R}_2 := (\vec{\rho}, Z_2)$. Using the cylindrical symmetry and the image boundary condition (45), the following expression is obtained:

$$J^{\tilde{L}}(Z, \alpha, t) = \frac{\pi e^{-i\omega_0 t}}{|\cos\alpha|} \int_{Z_1=0}^\infty \theta\left(\frac{Z-Z_1}{\cos\alpha}\right) \exp\left(\frac{Z_1-Z}{\ell \cos\alpha}\right) \int_{Z_2=0}^\infty \int_{\rho=0}^\infty \int_{\phi=0}^{2\pi} |E(\vec{\rho}, Z_2)|^2 \times \quad (55) \\ \times \left[\tilde{L}(\sqrt{\rho^2 + (Z_1-Z_2)^2}, t) - \tilde{L}(\sqrt{\rho^2 + (Z_1+Z_2+2Z_0)^2}, t) \right] \rho d\rho d\phi dZ_2 dZ_1.$$

Referring to the result (39) and assuming, that the input wave is a plane wave and its k -vector is oriented to \vec{OZ} , ($\vec{k}_0 = (0, 0, k_0)$) i.e. $E(\vec{R}) := E_0 \exp(i\vec{k}_0 \cdot \vec{R} - \frac{Z}{\ell})$ for $Z \geq 0$, it follows that:

$$J^{\tilde{L}}(Z, \alpha, t) = \frac{2\pi^2 |E_0|^2 e^{-i\omega_0 t}}{|\cos\alpha|} \int_{Z_1=0}^\infty \theta\left(\frac{Z-Z_1}{\cos\alpha}\right) \exp\left(\frac{Z_1-Z}{\ell \cos\alpha}\right) \times \\ \times \int_{Z_2=0}^\infty \int_{\rho=0}^\infty \left\{ \mathcal{F}(g(t)) \left[\frac{\exp\left(-\sqrt{\rho^2 + (Z_1-Z_2)^2} \frac{u}{\ell}\right)}{\sqrt{\rho^2 + (Z_1-Z_2)^2} \ell^3} \right] - \mathcal{F}(g(t)) \left[\frac{\exp\left(-\sqrt{\rho^2 + (Z_1+Z_2+2Z_0)^2} \frac{u}{\ell}\right)}{\sqrt{\rho^2 + (Z_1+Z_2+2Z_0)^2} \ell^3} \right] \right\} \rho d\rho dZ_2 dZ_1.$$

Now let us introduce dimensionless variables:

$$a := \frac{Z_1}{\ell} \quad b := \frac{Z_2}{\ell} \quad h := \frac{Z}{\ell}. \quad (56)$$

Since $\mathcal{F}(g(t))$ is a linear integral operator, it may be writ-

ten as

$$J^{\tilde{L}}(h, \alpha, t) = 4\pi^2 |E_0|^2 e^{-i\omega_0 t} \mathcal{F}(g(t)) [H^{\tilde{L}}(u, h, \alpha)], \quad (57)$$

where $H^{\tilde{L}}$ is defined by

$$H^{\tilde{L}}(u, h, \alpha) := \frac{1}{2|\cos\alpha|} \int_{a=0}^{\infty} \Theta\left(\frac{h-a}{\cos\alpha}\right) \exp\left(\frac{a-h}{\cos\alpha}\right) \int_{b=0}^{\infty} e^{-b} \times \quad (58)$$

$$\times \int_{\rho=0}^{\infty} \left[\frac{\exp\left(-\sqrt{\rho^2+(a-b)^2} u\right)}{\sqrt{\rho^2+(a-b)^2}} - \frac{\exp\left(-\sqrt{\rho^2+(a+b+2M)^2} u\right)}{\sqrt{\rho^2+(a+b+2M)^2}} \right] \rho d\rho db da$$

This integral can be calculated analytically and the final result is:

$$H^{\tilde{L}}(u, h, \alpha) = \frac{e^{-uh} - \theta(\cos\alpha) e^{-\frac{h}{\cos\alpha}}}{(1+u)(1-u\cos\alpha)} \left(\frac{\cos\alpha}{\cos\alpha-1} + \frac{1-e^{-2Mu}}{2u} \right) + \frac{e^{-uh} - e^{-h}}{1-\cos\alpha}. \quad (59)$$

Here h is the distance from the surface to the point, at which the intensity is measured, in units of *total mean free path*. Substituting (59) in (57) we get our final result for the incoherent multiple scattering intensity:

$$J^{\tilde{L}}(h, \alpha, t) = 4\pi^2 |E_0|^2 e^{-i\omega_0 t} \left[\frac{2\chi^2(t) H^{\tilde{L}}(\chi(t), h, \alpha)}{(1-\chi^2(t))^{-1} - g^{-1}(t)} + \int_1^{\infty} \frac{H^{\tilde{L}}(u, h, \alpha) du}{\left(g^{-1}(t) - \frac{1}{2u} \ln \frac{u+1}{u-1}\right)^2 + \frac{\pi^2}{4u^2}} \right] \quad (60)$$

The connection between $\chi(t)$ and $g(t)$ was defined by (38).

For the stationary case ($f(t)=1$) without absorption ($g(t)=f(t)$) from (57) and (60) it follows:

$$J^{\tilde{L}}(h, \alpha, t) = 4\pi^2 |E_0|^2 e^{-i\omega_0 t} \mathcal{F}(1) [H^{\tilde{L}}(u, h, \alpha)] = 4\pi^2 |E_0|^2 e^{-i\omega_0 t} \left[3 H^{\tilde{L}}(0, h, \alpha) + \int_1^{\infty} \frac{H^{\tilde{L}}(u, h, \alpha) du}{\left(1 - \frac{1}{2u} \ln \frac{u+1}{u-1}\right)^2 + \frac{\pi^2}{4u^2}} \right] \quad (61)$$

It is easy to obtain the single scattering intensity following the proposed analytical procedure – one must simply exchange the propagator \tilde{L} under the integral (50) with the single scattering propagator (see Appendix 4).

der type diagrams with exception of the first one. The relation between the two types of diagrams is:

VI. TIME REVERSAL INVARIANCE AND MULTIPLE COHERENT INTENSITY.

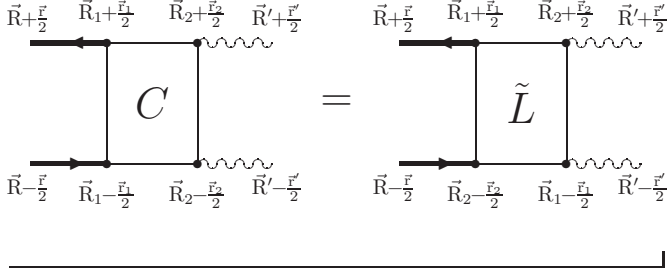
For a medium invariant under time-reversal all maximally-crossed diagrams may be expressed by lad-

$$C(\vec{R}_1, \vec{R}_2; \vec{r}_1, \vec{r}_2) = \tilde{L}\left(\frac{\vec{R}_1 + \vec{R}_2}{2} + \frac{\vec{r}_1 - \vec{r}_2}{4}, \frac{\vec{R}_1 + \vec{R}_2}{2} - \frac{\vec{r}_1 - \vec{r}_2}{4}; \vec{R}_1 - \vec{R}_2 + \frac{\vec{r}_1 + \vec{r}_2}{2}, \vec{R}_2 - \vec{R}_1 + \frac{\vec{r}_1 + \vec{r}_2}{2}\right) \quad (62)$$

The coherent scattering propagator may be replaced by the propagator corresponding to the ladder diagrams, but with variables as determined by the time-reversing

operation. Since the normal form of ladder diagrams is much more appropriate for calculation of the intensity, there is a necessity to make a **second operation of time**

reversal in order to express the coherent intensity by the usual ladder propagator. Doing this we have to change the variables in the expression for the coherent intensity. In the language of diagrams the coherent intensity is connected with the sum of ladder diagrams as follows:



For the coherent correlation of the scattered field function it follows that:

$$\begin{aligned} \Gamma_C(\vec{R}, \vec{r}, t) &= \tag{63} \\ &= e^{-i\omega_0 t} \int D\left(\vec{R} - \vec{R}_1 + \frac{\vec{r} - \vec{r}_1}{2}\right) D^*\left(\vec{R} - \vec{R}_2 - \frac{\vec{r} - \vec{r}_2}{2}\right) \tilde{L}(\vec{R}_1, \vec{R}_2, \vec{r}_1, \vec{r}_2; t) E\left(\vec{R}_2 + \frac{\vec{r}_2}{2}\right) E^*\left(\vec{R}_1 - \frac{\vec{r}_1}{2}\right) d^3\vec{R}_1 d^3\vec{R}_2 d^3\vec{r}_1 d^3\vec{r}_2 \end{aligned}$$

Because of the singularity of the propagator \tilde{L} , the value of the integral is determined by the range of integration, for which $\vec{R}_1 \approx \vec{R}_2$. Therefore we may use Fraunhofer approximation with respect to the difference $\vec{R}_1 - \vec{R}_2$:

$$D\left(\vec{R} - \vec{R}_1 + \frac{\vec{r} - \vec{r}_1}{2}\right) = D\left(\vec{R} - \vec{R}_+ - \frac{\vec{R}_-}{2} + \frac{\vec{r} - \vec{r}_1}{2}\right) \approx D(\vec{R} - \vec{R}_+) \exp\left(\frac{ik_0}{2} \vec{S}_{RR_+} \cdot (\vec{r} - \vec{r}_1 - \vec{R}_-)\right),$$

$$\begin{aligned} \text{where } \vec{R}_+ &:= \frac{\vec{R}_1 + \vec{R}_2}{2} & \text{or } \vec{R}_+ &:= (X_+, Y_+, Z_+) := \left(\frac{X_1 + X_2}{2}, \frac{Y_1 + Y_2}{2}, \frac{Z_1 + Z_2}{2}\right) \\ \vec{R}_- &:= \vec{R}_1 - \vec{R}_2 & \text{or } \vec{R}_- &:= (X_-, Y_-, Z_-) := (X_1 - X_2, Y_1 - Y_2, Z_1 - Z_2) \end{aligned}$$

If we substitute the last expression into the (63) and after integrations over $d^3\vec{r}_1$ and $d^3\vec{r}_2$ we get the expression:

$$\begin{aligned} \Gamma_C(\vec{R}, \vec{r}, t) &\approx \tag{64} \\ &\approx |E_0|^2 e^{-i\omega_0 t} \int \exp\left(ik_0 \vec{S}_{RR_+} \cdot \vec{r}\right) |D(\vec{R} - \vec{R}_+)|^2 \tilde{L}(\vec{R}_1, \vec{R}_2; t) \exp\left(-\frac{Z_+}{\ell}\right) \exp\left[-ik_0(\vec{S}_{RR_+} + \vec{S}_Z) \cdot \vec{R}_-\right] d^3\vec{R}_1 d^3\vec{R}_2, \end{aligned}$$

where \approx denotes s -wave approximation for \tilde{L} . Again converting this to its Fourier conjugated function with respect to \vec{r} , we obtain:

$$\Gamma_C(\vec{R}, \vec{k}, t) = \frac{\pi}{2} |E_0|^2 e^{-i\omega_0 t} \int \delta(\vec{k} - k_0 \vec{S}_{RR_+}) \frac{\exp\left(\frac{-|\vec{R} - \vec{R}_+|}{\ell}\right)}{(\vec{R} - \vec{R}_+)^2} \tilde{L}(\vec{R}_1, \vec{R}_2; t) \exp\left(\frac{-Z_+}{\ell}\right) \exp\left[ik_0(\vec{S}_{RR_+} + \vec{S}_Z) \cdot \vec{R}_-\right] d^3\vec{R}_1 d^3\vec{R}_2, \tag{65}$$

where:

$$\delta(k\vec{S} - k_0\vec{S}_{RR_+}) = \begin{cases} \frac{(Z-Z_+)^2}{k_0^2 |\cos\alpha|^3} \delta(k - k_0) \delta(X_+ + \text{tg}\alpha(Z - Z_+)) \delta(Y_+) \theta\left(\frac{Z-Z_+}{\cos\alpha}\right) & ; \alpha \neq \pi/2 \\ \frac{X_+^2}{k_0^2} \delta(k - k_0) \delta(Y_+) \delta(Z - Z_+) \theta(-X_+) & ; \alpha = \pi/2 \end{cases} \tag{66}$$

As in the case of incoherent scattering eqs. (51)-(55) we can obtain the intensity in the point $R = (0, 0, Z)$ for a given direction $\vec{S} = (\sin\alpha, 0, \cos\alpha)$:

$$\begin{aligned} J^C(Z, \alpha, t) &= \frac{\pi e^{-i\omega_0 t}}{|\cos\alpha|} \int_{Z_+ = 0}^{\infty} \theta\left(\frac{Z - Z_+}{\cos\alpha}\right) \exp\left(\frac{Z_+ - Z}{\ell \cos\alpha} - \frac{Z_+}{\ell}\right) \int_{Z_- = -2Z_+}^{+2Z_+} \exp[-ik_0(1 + \cos\alpha)Z_-] \times \tag{67} \\ &\times \int_{\rho \in \mathbb{R}^2} e^{-i\vec{k}_\perp \cdot \vec{\rho}} \left[\tilde{L}(\sqrt{\rho^2 + Z_-^2}, t) - \tilde{L}(\sqrt{\rho^2 + (2Z_+ + 2Z_0)^2}, t) \right] d^2\vec{\rho} dZ_- dZ_+. \end{aligned}$$

Similarly to eq. (57), we can write:

$$J^C(h, \alpha, t) = 8\pi^2 |E_0|^2 e^{-i\omega_0 t} \mathcal{F}(g(t)) [H^C(u, h, \alpha)], \quad (68)$$

where H^C is defined by

$$H^C(u, h, \alpha) := \frac{1}{2|\cos\alpha|} \int_{a=0}^{\infty} \Theta\left(\frac{h-a}{\cos\alpha}\right) \exp\left(\frac{a-h}{\cos\alpha} - a\right) \int_{b=-2a}^{2a} \exp[-ik_0\ell(1+\cos\alpha)b] \quad (69)$$

$$\int_{\rho=0}^{\infty} e^{-i\vec{k}_{\perp} \cdot \vec{\rho}} \left[\frac{\exp(-\sqrt{\rho^2+b^2}u)}{\sqrt{\rho^2+b^2}} - \frac{\exp(-\sqrt{\rho^2+(2a+2M)^2}u)}{\sqrt{\rho^2+(2a+2M)^2}} \right] \rho d\rho db da$$

If we introduce the notations $\xi(u) := 2\sqrt{(k_0\ell\sin\alpha)^2+u^2}$, $\eta := 2k_0\ell(1+\cos\alpha)$ we get the following expression for H^C :

$$H^C(u, h, \alpha) = \frac{1}{\xi^2 + \eta^2} \left\{ \frac{e^{-h} - \theta(\cos\alpha)e^{-\frac{h}{\cos\alpha}}}{1 - \cos\alpha} - \frac{e^{-(1+\xi)h} [(1 - (1+\xi)\cos\alpha) \cos(\eta h) + \eta \cos\alpha \sin(\eta h)] - \theta(\cos\alpha)e^{-\frac{h}{\cos\alpha}}}{(1 - (1+\xi)\cos\alpha)^2 + (\eta \cos\alpha)^2} + \right. \quad (70)$$

$$\left. + \left[\frac{\xi^2 + \eta^2}{\xi} (1 - e^{-M\xi}) - \xi \right] \frac{e^{-(1+\xi)h} [(1 - (1+\xi)\cos\alpha) \frac{\sin(\eta h)}{\eta} - \cos\alpha \cos(\eta h)] + \cos\alpha \theta(\cos\alpha)e^{-\frac{h}{\cos\alpha}}}{(1 - (1+\xi)\cos\alpha)^2 + (\eta \cos\alpha)^2} \right\}$$

Finally for the coherent multiple scattering intensity we obtain:

$$J^C(h, \alpha, t) = 8\pi^2 |E_0|^2 e^{-i\omega_0 t} \left[\frac{2\chi^2(t) H^C(\chi(t), h, \alpha)}{(1 - \chi^2(t))^{-1} - g^{-1}(t)} + \int_1^{\infty} \frac{H^C(u, h, \alpha) du}{\left(g^{-1}(t) - \frac{1}{2u} \ln \frac{u+1}{u-1}\right)^2 + \frac{\pi^2}{4u^2}} \right] \quad (71)$$

The connection between χ and g is defined by eq.(38). Following eq.(68) and eq.(71) the coherent intensity for the stationary case without absorption is obtained :

$$J^C(h, \alpha, t) = 8\pi^2 |E_0|^2 e^{-i\omega_0 t} \mathcal{F}(1) [H^C(u, h, \alpha)] = 8\pi^2 |E_0|^2 e^{-i\omega_0 t} \left[3 H^C(0, h, \alpha) + \int_1^{\infty} \frac{H^C(u, h, \alpha) du}{\left(1 - \frac{1}{2u} \ln \frac{u+1}{u-1}\right)^2 + \frac{\pi^2}{4u^2}} \right] \quad (72)$$

The summary scattering intensity is represented on Fig. 4 and the single scattering intensity on Fig. 5.

In these cylindrical plots the polar variable corresponds to the scattering angle, the radial variable corresponds to the scattering intensity, and the vertical variable is the depth of observation in dimensionless units (*elastic mean free path*). $k\ell = 100$ Forward direction is in the right side of the plots.

VII. PARTIAL INTENSITIES.

In this section we shall estimate the validity of the diffusion approximation in different orders of multiple scattering. Our goal is to find a physically well-motivated explanation for the failure of the diffusion approximation in the case of large scattering angles.

We have shown (eqs.(31),(33) and (36)) that the Fourier transform of the ladder propagator are a convergent infinite geometric series. It is therefore possible to study the scattered intensity as a function of the order of scattering. It means that the coherent and incoherent intensities may be expanded into the orders of multiple scattering:

$J^{\tilde{L}} = \sum_{n=2}^{\infty} J_n^L$; $J^C = \sum_{n=2}^{\infty} J_n^C$, where J_n^L and J_n^C denote, respectively, the partial incoherent and coherent intensities of n^{th} order.

To obtain the partial intensities, we start from the expressions (55) and (67), in which $\tilde{L}(\vec{\rho}, Z; t)$ is represented by its Fourier transforms:

$$J^{\tilde{L}}(Z, \alpha, t) = \frac{|E_0|^2 e^{-i\omega_0 t}}{4|\cos\alpha|} \int_{Z_1=0}^{\infty} \theta\left(\frac{Z-Z_1}{\cos\alpha}\right) \exp\left(\frac{Z_1-Z}{\ell \cos\alpha}\right) \int_{Z_2=0}^{\infty} e^{-\frac{Z_2}{\ell}} \int_{\vec{\rho} \in \mathbb{R}^2} e^{-i\vec{k}_{\perp} \cdot \vec{\rho}} \times \quad (73)$$

$$\int_{K_z=-\infty}^{\infty} \int_{\vec{K}_{\perp} \in \mathbb{R}^2} e^{i\vec{K}_{\perp} \cdot \vec{\rho}} \left[e^{iK_z(Z_1-Z_2)} - e^{iK_z(Z_1+Z_2+2Z_0)} \right] \tilde{L}\left(\sqrt{K_{\perp}^2 + K_z^2}, t\right) \frac{d^2\vec{K}_{\perp}}{(2\pi)^2} dK_z d^2\vec{\rho} dZ_2 dZ_1$$

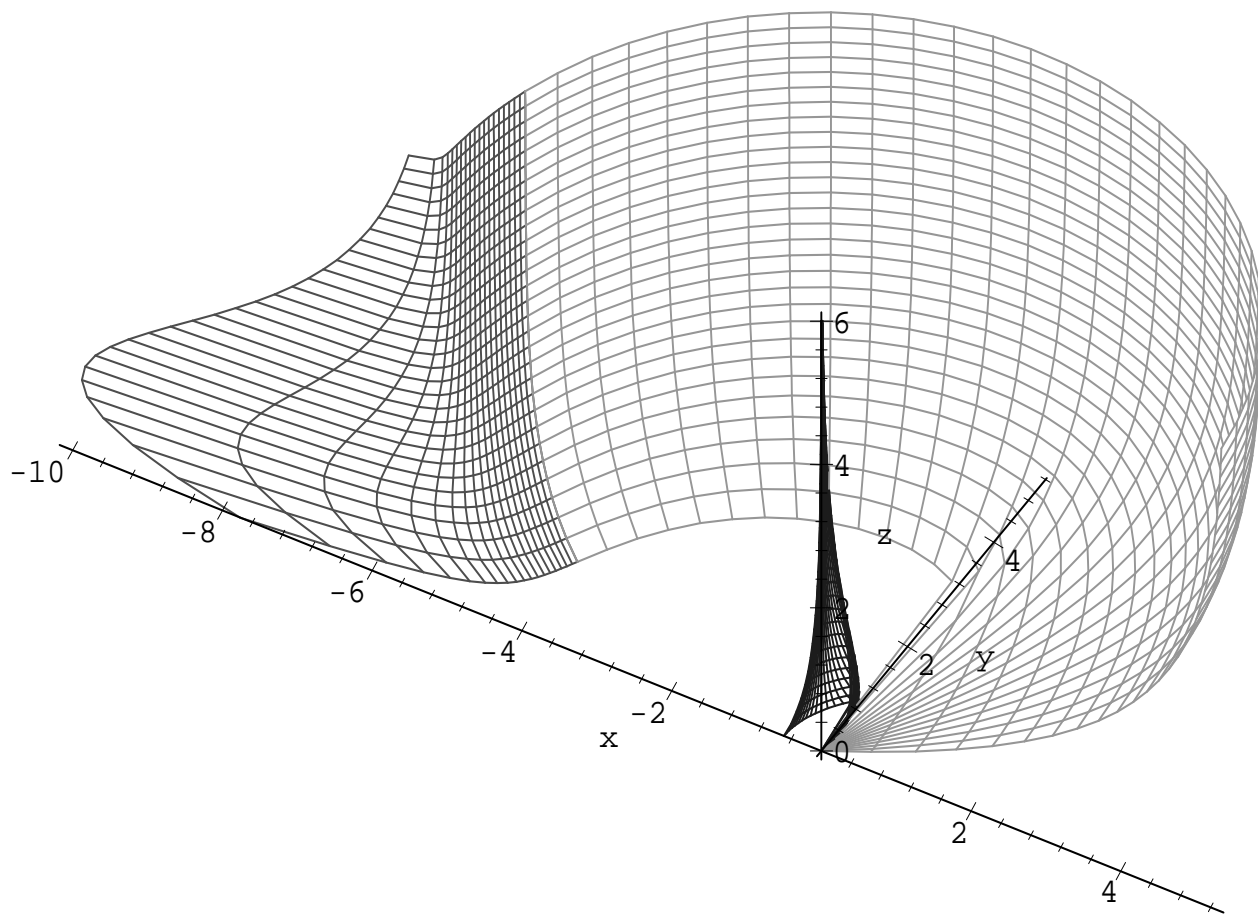


FIG. 4: Multiple scattering intensity.

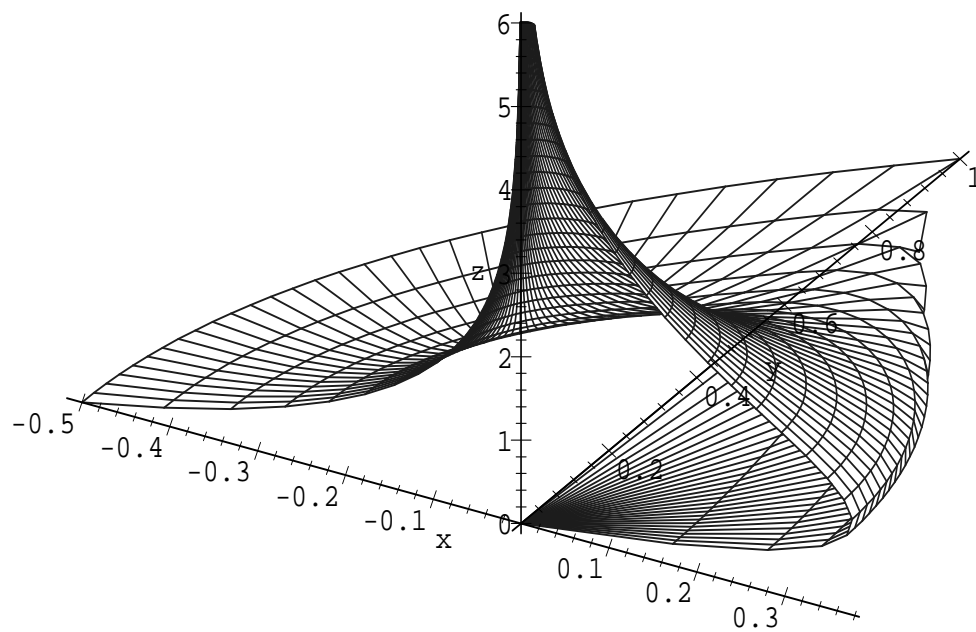


FIG. 5: Single scattering intensity.

$$J^C(Z, \alpha, t) = \frac{|E_0|^2 e^{-i\omega_0 t}}{4|\cos\alpha|} \int_{Z_+=0}^{\infty} \theta\left(\frac{Z-Z_+}{\cos\alpha}\right) \exp\left(\frac{Z_+-Z}{\ell \cos\alpha} - \frac{Z_+}{\ell}\right) \int_{Z_-=-2Z_+}^{2Z_+} \exp[-ik_0(1+\cos\alpha)Z_-] \times \quad (74)$$

$$\int_{\vec{p} \in \mathbb{R}^2} e^{-i\vec{k}_\perp \varepsilon \cdot \vec{p}} \int_{K_z=-\infty}^{\infty} \int_{\vec{K}_\perp \in \mathbb{R}^2} e^{i\vec{K}_\perp \cdot \vec{p}} \left[e^{iK_z Z_-} - e^{i2K_z(Z_++Z_0)} \right] \tilde{L}\left(\sqrt{K_\perp^2 + K_z^2}, t\right) \frac{d^2 \vec{K}_\perp}{(2\pi)^2} dK_z d^2 \vec{p} dZ_- dZ_+,$$

where $|\vec{k}_\perp| := k_0 \sin\alpha$. Performing integrations, first with respect to $d^2 \vec{p}$ and $d^2 \vec{K}_\perp$ and after that with respect to $dZ_2 dZ_1$ in (73), and $dZ_- dZ_+$ in (74), it follows:

$$J^{\tilde{L}}(h, \alpha, t) = \frac{|E_0|^2 e^{-i\omega_0 t}}{4} \int_{-\infty}^{+\infty} \ell \tilde{L}\left(\frac{p}{\ell}, t\right) \frac{e^{ihp} - \theta\left(\frac{\pi}{2} - \alpha\right) \exp\left(-\frac{h}{\cos\alpha}\right)}{1 + ip \cos\alpha} \left(\frac{1}{1 + ip} - \frac{e^{2iMp}}{1 - ip} \right) dp \quad (75)$$

$$J^C(h, \alpha, t) = \quad (76)$$

$$= \frac{|E_0|^2 e^{-i\omega_0 t - h}}{2|\cos\alpha|} \int_{-\infty}^{+\infty} \ell \tilde{L}\left(\frac{\sqrt{q^2 + v^2}}{2\ell}, t\right) \left[\frac{\cos((q-\eta)h) + \frac{\beta}{q-\eta} \sin((q-\eta)h)}{(q-\eta)^2 + \beta^2} - e^{i(h+M)q} \frac{\cos(\eta h) + \frac{(\beta-iq)}{\eta} \sin(\eta h)}{(\beta-iq)^2 + \eta^2} \right] dq,$$

$$\text{where } h := \frac{Z}{\ell}, \quad p := K_z \ell, \quad q := 2p, \quad v := 2k_0 \ell \sin\alpha, \quad \beta := 1 + \frac{1}{\cos\alpha}, \quad \eta := 2k_0 \ell (1 + \cos\alpha).$$

As we already mentioned the exact time-dependent ladder propagator is geometric series with base $g(t) \frac{\text{arctg}(p)}{p}$:

$$\tilde{L}\left(\frac{p}{\ell}, t\right) = \frac{4\pi}{\ell} \frac{g^2(t) \frac{\text{arctg}(p)}{p}}{1 - g(t) \frac{\text{arctg}(p)}{p}} = \frac{4\pi}{\ell} g(t) \sum_{n=1}^{\infty} \left(g(t) \frac{\text{arctg}(p)}{p} \right)^n \quad (77)$$

To compare the exact partial intensities with these, corresponding to the diffusion approximation, we should find the correct representation of the diffusion propagator as convergent geometric series. In the standard approach^{11,16,17,19,20}, the diffusion propagator is considered as obtained by the exact ladder propagator taking only the first order with respect to p^2 for $|p| \ll 1$ in the expansion of $\text{arctg}(p)/p$, so that:

$$g(t) \frac{\text{arctg}(p)}{p} \rightarrow 1 - \frac{1}{3}(\chi_1^2(t) + p^2) \quad (78)$$

and

$$\frac{g(t)}{1 - g(t) \frac{\text{arctg}(p)}{p}} \rightarrow \frac{3g(t)}{\chi_1^2(t) + p^2} \stackrel{?}{=} 3g(t) \sum_{n=0}^{\infty} (1 - \chi_1^2(t) - p^2)^n, \quad (79)$$

for $|p| < \sqrt{1 - \chi_1^2(t)}$, $\chi_1(t) \ll 1$.

Thus it is not clear in which way should be performed the Fourier transformation over p because of the restriction to the p -values ($|p| \ll 1$). The above mentioned approximation is used in paper¹⁶ in order to be obtained the partial coherent intensities in the stationary case without absorption ($\chi=0$). To obtain the different orders of

scattering one must take the Fourier transform of the different addends of $\sum_{n=0}^{\infty} (1-p^2)^n$. Since the convergence radius of the sum in (79), imposes a restriction to the p -values ($|p| < 1$), we face with the cut-off of the integral limits: $\int_{-\infty}^{+\infty} dp \rightarrow \int_{|p| < 1} dp$. Therefore, the partial coherent intensities turn out to be zero outside the interval $0 \leq \pi - \alpha < 1/k\ell$. In contrast, the total coherent intensity, which has been calculated after integrating over all real p , does not become zero outside the polar angle interval. So that the summation of all scattering orders can not reproduce the total coherent intensity. In paper¹⁶ this cut-off of the partial intensities is interpreted as a feature of the diffusion approximation, but in our opinion it is **an additional systematical error itself, which does not originate from the diffusion approximation**. This strange situation can be escaped by a rather different choice of the geometric series base, standing on the following considerations:

1. **The single-scattering has not to be included in the diffusion propagator**¹¹.

2. The diffusion approximation for ladder propagator describes the asymptotic behaviour of $\tilde{L}(R; t)$ for large values of R and corresponds simply to the first term of the expression(39). **So the diffusion propagator in con-**

jugated variables must be considered as a Fourier transform of the first term of (39), but not as an approximation for the Fourier transform of the

exact expression (79), when $|p| \ll 1$. Namely (39) could be written as:

$$\tilde{L}(R; t) = \frac{4\pi}{\ell^4} \int \frac{g^2(t) \frac{\text{arctg}(p)}{p}}{1 - g(t) \frac{\text{arctg}(p)}{p}} e^{i\vec{p} \cdot \frac{\vec{R}}{\ell}} \frac{d^3\vec{p}}{(2\pi)^3} = \frac{4\pi}{\ell^4} \int \frac{A(\chi(t))}{p^2 + \chi^2(t)} e^{i\vec{p} \cdot \frac{\vec{R}}{\ell}} \frac{d^3\vec{p}}{(2\pi)^3} + \frac{1}{R \ell^3} \int_1^\infty \frac{\exp(-R \frac{u}{\ell}) du}{\left(g^{-1}(t) - \frac{1}{2u} \ln \frac{u+1}{u-1}\right)^2 + \frac{\pi^2}{4u^2}}$$

3. The diffusion propagator in p -representation must be an infinite geometric sum with series base between 0 and 1 not only for small p -values, but also for all real p -values. This allows us to take Fourier transform of $L_n(p/\ell, t)$ without imposing restrictions to the integral limits. In the context of above mentioned arguments, the exchange $g(t) \frac{\text{arctg}(p)}{p} \rightarrow \frac{B}{B+p^2+\chi^2(t)}$ gives the most proper choice of series base. In contrast to the standard approach the last one is not an approximation for the exact series base. Then

$$\begin{aligned} \frac{g^2(t) \frac{\text{arctg}(p)}{p}}{1 - g(t) \frac{\text{arctg}(p)}{p}} &= g(t) \sum_{n=1}^{\infty} \left(g(t) \frac{\text{arctg}(p)}{p} \right)^n \xrightarrow{\text{diff}} \quad (80) \\ &\xrightarrow{\text{diff}} \frac{A}{p^2 + \chi^2(t)} = \frac{A}{B} \sum_{n=1}^{\infty} \left(\frac{B}{B + p^2 + \chi^2(t)} \right)^n, \end{aligned}$$

where A has already been defined in (39) and B is an arbitrary positive function, moreover it may depend on p .

4. To restrict the generality of B ($B := B(p, \chi)$), according to the correspondence between the two sums in (80), it should be determined B as $B := A(\chi(t))g^{-1}(t)$. Besides $g(t) \frac{\text{arctg}(p)}{p}$ and $\frac{B}{B+p^2+\chi^2(t)}$ have one and the same behaviour for p -values close to the complex singularities $\pm i\chi$ of the ladder propagator:

$$g(t) \frac{\text{arctg}(p)}{p} = 1 - \frac{g(t)}{A} (p^2 + \chi^2) + \text{higher orders } p^2 + \chi^2,$$

$$\frac{B}{B + p^2 + \chi^2(t)} = 1 - \frac{1}{B} (p^2 + \chi^2) + \text{higher orders } p^2 + \chi^2.$$

Furthermore, both series bases vanish for infinite $|p|$.

The above considerations lead us to the choice (80), which avoids any problems with the Fourier transformation. Moreover, we find decomposition of the diffusion propagator to the different orders of scattering not only for large EDL (small χ), where χ is given by its first order approximated representation $\chi_1(t) := \sqrt{3g^{-1}(t)-3}$, but also for any χ , which is a solution of the equation (38). Further we are going to demonstrate that the sum of the partial intensities tends really to the total scattered intensity when the number of included scattering orders increases significantly. In addition, for fixed number of included scatterings, the sum approaches to the total intensity when the EDL increases.

A. Incoherent intensities.

Replacing the ladder propagator in (75) with $L_{n+1}(p; t) := (4\pi g(t)/\ell) (g(t) \text{arctg } p/p)^n$, we will get the $(n+1)$ -th partial intensity:

$$J_{n+1}^L(h, \alpha, t) = \pi |E_0|^2 e^{-i\omega_0 t} g(t) \int_{-\infty}^{+\infty} \left(g(t) \frac{\text{arctg}(p)}{p} \right)^n \frac{e^{ihp} - \theta\left(\frac{\pi}{2} - \alpha\right) \exp\left(-\frac{h}{\cos\alpha}\right)}{1 + ip \cos\alpha} \left(\frac{1}{1 + ip} - \frac{e^{2iMp}}{1 - ip} \right) dp, \quad (81)$$

and after the exchange $\tilde{L}(p; t) \rightarrow L_{n+1}^{\text{diff}}(p, t) := (4\pi g(t)/\ell) (B/(B+p^2+\chi^2(t)))^n$ in (81), we will have the partial intensities in diffusion approximation:

$$J_{n+1}^{\text{diff}}(h, \alpha, t) = \pi |E_0|^2 e^{-i\omega_0 t} g(t) \int_{-\infty}^{+\infty} \left(\frac{B}{B + p^2 + \chi^2(t)} \right)^n \frac{e^{ihp} - \theta\left(\frac{\pi}{2} - \alpha\right) \exp\left(-\frac{h}{\cos\alpha}\right)}{1 + ip \cos\alpha} \left(\frac{1}{1 + ip} - \frac{e^{2iM_{as}p}}{1 - ip} \right) dp, \quad (82)$$

Upper expression can be evaluate analytically as an contour integral in complex plane, using the theorem of residuums, so we get:

$$J_{n+1}^{\text{diff}}(h, \alpha, t) = 2\pi^2 |E_0|^2 e^{-i\omega_0 t} g(t) \left\{ \left(\frac{B}{u^2 - 1} \right)^n \frac{e^{-h} - \theta\left(\frac{\pi}{2} - \alpha\right) \exp\left(-\frac{h}{\cos\alpha}\right)}{1 - \cos\alpha} + \right. \quad \left. u := \sqrt{B + \chi_1^2(t)} \right\} \quad (83)$$

$$\begin{aligned}
& + B^n \sum_{k=1}^n \binom{2n-k-1}{n-1} (2u)^{k-2n} \sum_{m=0}^{k-1} \frac{1}{m!} \left[\frac{\left(\frac{\cos\alpha}{u \cos\alpha - 1}\right)^{k-m} - \left(\frac{1}{u-1}\right)^{k-m}}{1 - \cos\alpha} \left(h^m e^{-uh} - \theta(-m) \theta\left(\frac{\pi}{2} - \alpha\right) \exp\left(-\frac{h}{\cos\alpha}\right) \right) + \right. \\
& \left. + \frac{\left(\frac{\cos\alpha}{u \cos\alpha - 1}\right)^{k-m} - \left(\frac{1}{u+1}\right)^{k-m}}{1 + \cos\alpha} \left((h + 2M_{as})^m e^{-u(h+2M_{as})} - (2M_{as})^m e^{-2M_{as}u} \theta\left(\frac{\pi}{2} - \alpha\right) \exp\left(-\frac{h}{\cos\alpha}\right) \right) \right] \Bigg\} .
\end{aligned}$$

For first order approximation $\chi(t) \approx \chi_1(t) := \sqrt{3g^{-1}(t)-3}$, $A(\chi(t)) \approx A_1(\chi(t)) := 3$ are given in ap-

pendix, for the angles $\alpha = \{0, \pi/2, \pi\}$ consequently (105), (106), (107).

From 2 to 10 order incoherent scattering intensity for forward (Fig. 6a), backward (Fig. 6b) and perpendicular (Fig. 6c) direction are graphically represented, as functions of depth calculated by formula (83) for stationary case $B=3$. There is a small difference between the results coming from (81) and these one's given by (83), which becomes negligible for depths of order several mean free path.

B. Coherent intensities.

Replacing the ladder propagator in (76) with $L_{n+1}(\tilde{p}; t) := (4\pi g(t)/\ell) (g(t) \operatorname{arctg} \tilde{p}/\tilde{p})^n$, where $\tilde{p} := \sqrt{q^2 + v^2}/2$, we will get the $(n+1)$ -th partial intensity:

$$\begin{aligned}
J_{n+1}^C(h, \alpha, t) &= \frac{2\pi g(t) |E_0|^2 e^{-i\omega_0 t - h}}{|\cos\alpha|} \times \\
&\times \int_{-\infty}^{+\infty} \left(g(t) \frac{\operatorname{arctg}(\sqrt{q^2 + v^2}/2)}{\sqrt{q^2 + v^2}/2} \right)^n \left[\frac{\cos((q-\eta)h) + \frac{\beta}{q-\eta} \sin((q-\eta)h)}{(q-\eta)^2 + \beta^2} - e^{i(h+M)q} \frac{\cos(\eta h) + \frac{(\beta-iq)}{\eta} \sin(\eta h)}{(\beta-iq)^2 + \eta^2} \right] dq,
\end{aligned} \tag{84}$$

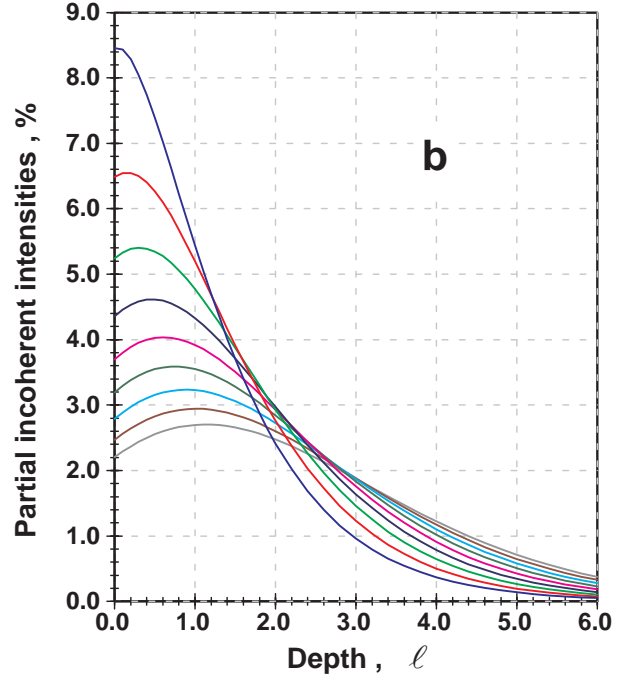
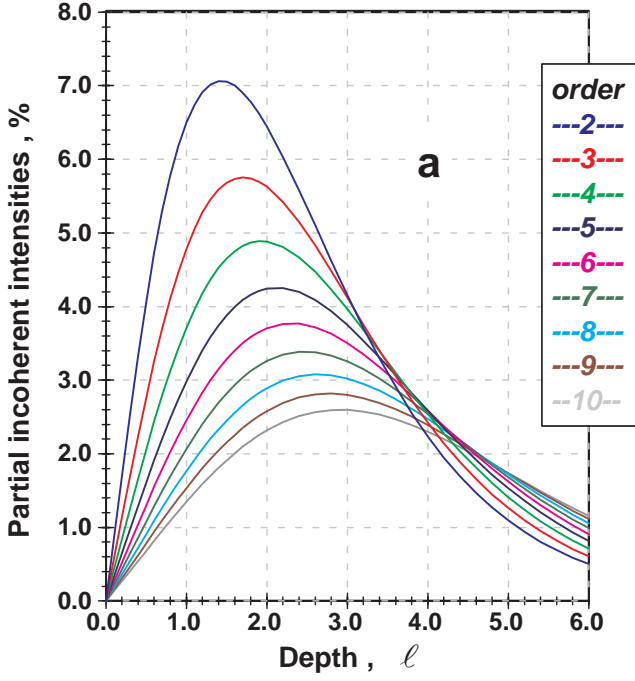
Following (80) it can be written:

$$\begin{aligned}
J_{n+1}^{C\text{diff}}(h, \alpha, t) &= \frac{2\pi g(t) |E_0|^2 e^{-i\omega_0 t - h}}{|\cos\alpha|} \times \\
&\times \int_{-\infty}^{+\infty} \left(\frac{4B}{4(B+\chi^2) + q^2 + v^2} \right)^n \left[\frac{\cos((q-\eta)h) + \frac{\beta}{q-\eta} \sin((q-\eta)h)}{(q-\eta)^2 + \beta^2} - e^{i(h+M_{as})q} \frac{\cos(\eta h) + (\beta-iq) \frac{\sin(\eta h)}{\eta}}{(\beta-iq)^2 + \eta^2} \right] dq
\end{aligned} \tag{85}$$

and for stationary case ($\chi(t)=0$, $B=3$)

$$\begin{aligned}
J_{n+1}^{C\text{diff}}(h, \alpha, t) &= \frac{2\pi g(t) |E_0|^2 e^{-i\omega_0 t - h}}{|\cos\alpha|} \times \\
&\times \int_{-\infty}^{+\infty} \left(\frac{12}{q^2 + v^2 + 12} \right)^n \left[\frac{\cos((q-\eta)h) + \frac{\beta}{q-\eta} \sin((q-\eta)h)}{(q-\eta)^2 + \beta^2} - e^{i(h+M_{as})q} \frac{\cos(\eta h) + (\beta-iq) \frac{\sin(\eta h)}{\eta}}{(\beta-iq)^2 + \eta^2} \right] dq
\end{aligned} \tag{86}$$

$$\begin{aligned}
J_{n+1}^{C\text{diff}}(h, \alpha, t) &= \frac{2\pi^2 g(t) |E_0|^2 e^{-i\omega_0 t - h}}{|\cos\alpha| \beta} \left\{ \left(\frac{4B}{(\eta+i\beta)^2 + w^2} \right)^n e^{\beta h} + \left(\frac{B}{w^2} \right)^n \sum_{k=0}^{n-1} (2w)^{k+1} \binom{2n-2-k}{n-1} \times \right. \\
&\times \left[(-1)^k \sum_{m=0}^k \frac{h^m}{m!} e^{(w+i\eta)h} [(w+i\eta)^{m-k-1} - (w-\beta+i\eta)^{m-k-1}] - (-1)^m e^{-(w+i\eta)h} [(w+i\eta)^{m-k-1} - (w+\beta+i\eta)^{m-k-1}] \right] \\
&\left. - e^{-(h+M)w} \frac{\beta}{i\eta} \sum_{m=0}^k \frac{(h+M)^m}{m!} \left[\frac{e^{i\eta h}}{(\beta+w-i\eta)^{k-m+1}} - \frac{e^{-i\eta h}}{(\beta+w+i\eta)^{k-m+1}} \right] \right\}
\end{aligned} \tag{87}$$



| $\pi - \alpha$ [mrad] | $\sum_{n=2}^{30} J_n^C(\alpha)$ [%] | $J^C(\alpha)$ [%] | $\sum_{n=2}^{30} J_n^C(\alpha) / J^C(\alpha)$ [%] |
|--------------------------|--|----------------------|--|
| 0 | 60.1602 | 100 | 60.1602 |
| 0.1 | 58.6109 | 79.3561 | 73.8581 |
| 0.2 | 54.4049 | 64.1648 | 84.7894 |
| 0.3 | 48.6108 | 52.7181 | 92.2089 |
| 0.328259 | 46.8503 | 50 | 93.7007 |
| 0.4 | 42.3775 | 43.9175 | 96.4935 |
| 0.5 | 36.5173 | 37.0323 | 98.6094 |
| 0.6 | 31.4086 | 31.5630 | 99.5109 |
| 0.7 | 27.1179 | 27.1597 | 99.8459 |
| 0.8 | 23.5616 | 23.5719 | 99.9560 |
| 0.9 | 20.6147 | 20.6171 | 99.9885 |
| 1.0 | 18.1591 | 18.1596 | 99.9972 |

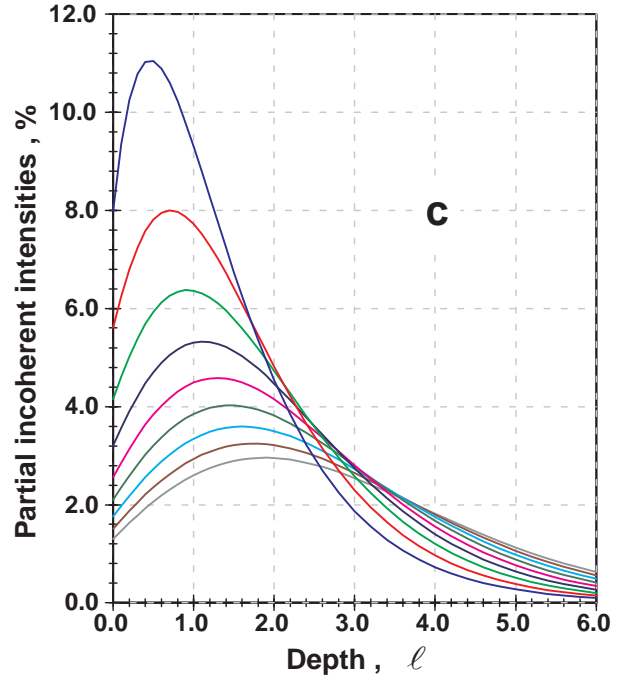


FIG. 6: Partial incoherent intensities for various depth for forward (6a), backward (6b) and perpendicular (6c) directions (100% corresponds to total incoherent intensity on the surface).

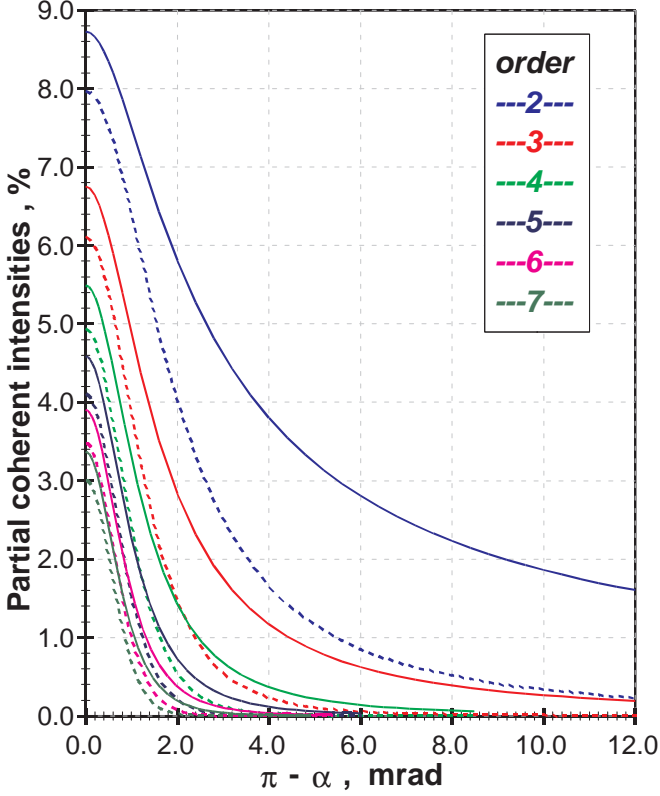


FIG. 7: The exact lineshapes represented by solid lines and the lineshapes for diffusion approximation, represented by dashed lines (100% corresponds to total coherent intensity on the surface).

The exact expressions (84) give us an opportunity to take into consideration the contributions of the different orders of multiple scattering. It affords us also illustrate the limits of applicability of the diffusion approximation for the different orders of scattering Fig. VII B.

| $\pi - \alpha$ [mrad] | $\sum_{n=2}^{10} J_n^C(\alpha)/J^C(\alpha)$ [%] | | | | |
|--------------------------|---|----------------|----------------|----------------|----------------|
| | $\chi = 0$ | $\chi = 0.01$ | $\chi = 0.1$ | $\chi = 0.2$ | $\chi = 0.5$ |
| 0.0 | 38.8935 | 39.8374 | 48.6249 | 58.7508 | 86.4635 |
| 0.1 | 48.4693 | 48.5190 | 52.6263 | 60.9547 | 86.9847 |
| 0.2 | 58.0091 | 58.0342 | 60.3816 | 66.2827 | 88.4047 |
| 0.3 | 66.9634 | 66.9796 | 68.5276 | 72.7159 | 90.3713 |
| 0.4 | 74.8999 | 74.9110 | 75.9879 | 78.9887 | 92.4898 |
| 0.5 | 81.5625 | 81.5704 | 82.3306 | 84.4765 | 94.4541 |
| 0.6 | 86.8802 | 86.8857 | 87.4206 | 88.9389 | 96.0933 |
| 0.7 | 90.9328 | 90.9366 | 91.3085 | 92.3661 | 97.3566 |
| 0.8 | 93.8955 | 93.8981 | 94.1527 | 94.8765 | 98.2711 |
| 0.9 | 95.9834 | 95.9852 | 96.1565 | 96.6431 | 98.9007 |
| 1.0 | 97.4086 | 97.4097 | 97.5232 | 97.8449 | 99.3168 |

| $\pi - \alpha, mrad$ | 2 order | 3 order | 4 order | 5 order | 6 order | 7 order | 8 order | 9 order | 10 order |
|----------------------|---------|---------|---------|---------|---------|---------|------------|-------------|--------------|
| 0 | 0.91352 | 0.90569 | 0.89992 | 0.89563 | 0.89347 | 0.89323 | 0.89444 | 0.89681 | 0.90625 |
| 0.6 | 0.89083 | 0.86237 | 0.83804 | 0.81649 | 0.79813 | 0.78263 | 0.76946 | 0.75833 | 0.75783 |
| 1.2 | 0.82067 | 0.73078 | 0.65418 | 0.58712 | 0.52865 | 0.47765 | 0.43297 | 0.39394 | 0.37374 |
| 1.8 | 0.72441 | 0.56627 | 0.44525 | 0.35067 | 0.27672 | 0.21888 | 0.17357 | 0.13834 | 0.12712 |
| 2.4 | 0.62918 | 0.4242 | 0.28784 | 0.19555 | 0.13297 | 0.09052 | 0.06172 | 0.04243 | 0.04917 |
| 3.0 | 0.54681 | 0.31814 | 0.18639 | 0.10935 | 0.06418 | 0.03769 | 0.02215 | 0.01323 | -0.05875 |
| 12 | 0.1598 | 0.02602 | 0.00425 | 0.00069 | 0.00007 | 0.00001 | 5.28693E-7 | -3.68948E-8 | -2.42003E-11 |

VIII. BACK TO THE DIFFUSION APPROXIMATION AND SMALL ANGLE ANALYSIS.

It is easy to obtain the results for incoherent and coherent scattering intensities in the diffusion approximation from eqs. (60) and (71). It is sufficient to take the first terms in eqs. (60) and (71) and after that to take into account the approximation $N=1$ eq. (43) in the diffusion

term, so $\chi \approx \chi_1$ and the incoherent intensity becomes:

$$J^{\bar{L}}(h, \alpha, t) = 6\pi^2 |E_0|^2 e^{-i\omega_0 t} H^{\bar{L}}(\chi_1(t), h, \alpha). \quad (88)$$

For coherent intensity the result is:

$$J^C(h, \alpha, t) = 24\pi^2 |E_0|^2 e^{-i\omega_0 t} H^C(\chi_1(t), h, \alpha). \quad (89)$$

As it is seen from the graphics (Fig. VII B), the diffusion approximation for the coherent backscattering gives a good description only in a narrow cone around $\alpha \approx \pi$.

In the region of the backscattering peak incoherent intensity is practically a constant. In most previous papers this has been understood without mentioning explicitly:

$$H^{\tilde{L}}(\chi_1(t), h, \alpha) \approx H^{\tilde{L}}(\chi_1(t), h, \pi) \quad (90)$$

Using the expression (59) and (71) for incoherent intensity in depth it can be seen that

$$J^{\tilde{L}}(h, \alpha, t) = 3\pi^2 |E_0|^2 e^{-i\omega_0 t} \left[\frac{e^{-\chi_1(t)h}}{(1+\chi_1(t))^2} \left(1 + \frac{1-e^{-2M\chi_1(t)}}{\chi_1(t)} \right) + e^{-\chi_1(t)h} + e^{-h} \right] \quad (91)$$

The simple approximated formulas for weak localization term can be obtained after substitution $\eta=0$ in (70). In the standard algebras(calculations) of the coherent in-

tensity expression, such an assumption is made before integration over $d^3\mathbf{R}^{19}$.

$$J^C(h, \alpha \approx \pi, t) \approx \frac{24\pi^2 |E_0|^2 e^{-i\omega_0 t}}{\xi^2} \left\{ \frac{e^{-h}}{2} - \frac{e^{-(1+\xi)h}}{2+\xi} \left[\xi e^{-M\xi} \left(h + \frac{1}{2+\xi} \right) + 1 \right] \right\}$$

Now let's take $h=0$ and we obtain the well known expressions for the incoherent and coherent scattering intensities on the surface.

$$J^{\tilde{L}}(0, \alpha, t) \approx \frac{3\pi^2 |E_0|^2 e^{-i\omega_0 t}}{(1+\chi_1(t))^2} (1+2M) \quad (92)$$

$$J^C(0, \alpha, t) \approx \frac{3\pi^2 |E_0|^2 e^{-i\omega_0 t}}{\left(1 + \sqrt{(k_0 \ell \sin \alpha)^2 + \chi_1^2(t)}\right)^2} \left[1 + \frac{1 - \exp\left(-2M \sqrt{(k_0 \ell \sin \alpha)^2 + \chi_1^2(t)}\right)}{\sqrt{(k_0 \ell \sin \alpha)^2 + \chi_1^2(t)}} \right] \quad (93)$$

IX. INTEGRAL SCATTERING INTENSITIES FOR VARIOUS DEPTHS IN THE STATIONARY CASE.

In some cases like these devoted to the investigations of the relationship between the impurities averaged perturbation theory and classical transport theory^{14,26,30}, the integral intensity over all directions must be included. However these considerations face some difficulties when one tries to take into account the weak localization effects. We have not intention to deal with this problem now. Independently it is interesting to know the difference between the integral scattering intensity in the diffusion approximation and this one determined by the expressions (61), (59), (72) and (70), so let's introduce the ratios:

$$R_L(h) := \frac{3 \int_0^\pi H^{\tilde{L}}(0, h, \alpha) \sin \alpha \, d\alpha}{\int_0^\pi \left[3 H^{\tilde{L}}(0, h, \alpha) + \int_1^\infty \frac{H^{\tilde{L}}(u, h, \alpha) \, du}{\left(1 - \frac{1}{2u} \ln \frac{u+1}{u-1}\right)^2 + \frac{\pi^2}{4u^2}} \right] \sin \alpha \, d\alpha} \quad (94)$$

$$R_C(h) := \frac{3 \int_0^{\alpha_0} H^C(0, h, \alpha) \sin \alpha \, d\alpha}{\int_0^{\alpha_0} \left[3 H^C(0, h, \alpha) + \int_1^\infty \frac{H^C(u, h, \alpha) \, du}{\left(1 - \frac{1}{2u} \ln \frac{u+1}{u-1}\right)^2 + \frac{\pi^2}{4u^2}} \right] \sin \alpha \, d\alpha} \quad (95)$$

As it was expected there is not any significant difference between the integral contribution of the first term, which corresponds to the diffusion approximation, and the second one in the (61). The relative integral contribu-

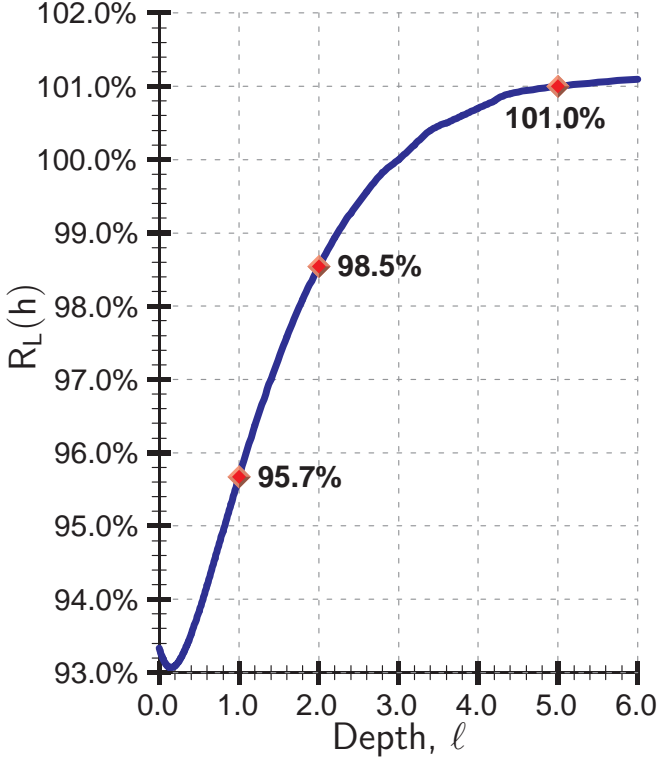


FIG. 8: Ratio $R_L(h)$ between the integral incoherent intensity given by the diffusion approximation and full integral incoherent intensity for various depths, where the integration is taken over 4π -steradians.

tion of the diffusion term is given by the ratio (94), graphically represented on the Fig. 8. As it is remarked above the lower order diagrams are not correctly accounted by diffusion approximation. Very far from the surface, where unscattered intensity is already vanished, the main contribution to the intensity is due to the very high order ladder diagrams. That's why in this case the diffusion approximation brings the exact result (see Fig. 8).

The similar results are obtained for the coherent case (ratio (95)) when the integration is taken over narrow cone around the backscattering peak ($\alpha_0 = 1/k\ell$). The numerical calculations represented on Fig. 9 show that for the characteristic polar angle interval ($[0, 1/k\ell]$) the diffusion approximation is permissible.

Unfortunately the **integral value of the coherent intensity is not concentrated only near the backscattering peak**. It is interesting that for the large polar angles the values of the function (72) are extremely low, and in spite of this **the main contribution in the integral coherent intensity comes from the integration outside the characteristic cone**. It is obviously from the numerical results (Fig. 9), where the integration is taken over all directions ($\alpha_0 = \pi$), that the contribution of the diffusion term in the coherent intensity (ratio (95)) is negligible. Moreover, as larger is the parameter $k\ell$ as lower is the integral contribution of the diffusion term to the whole integral intensity coming from

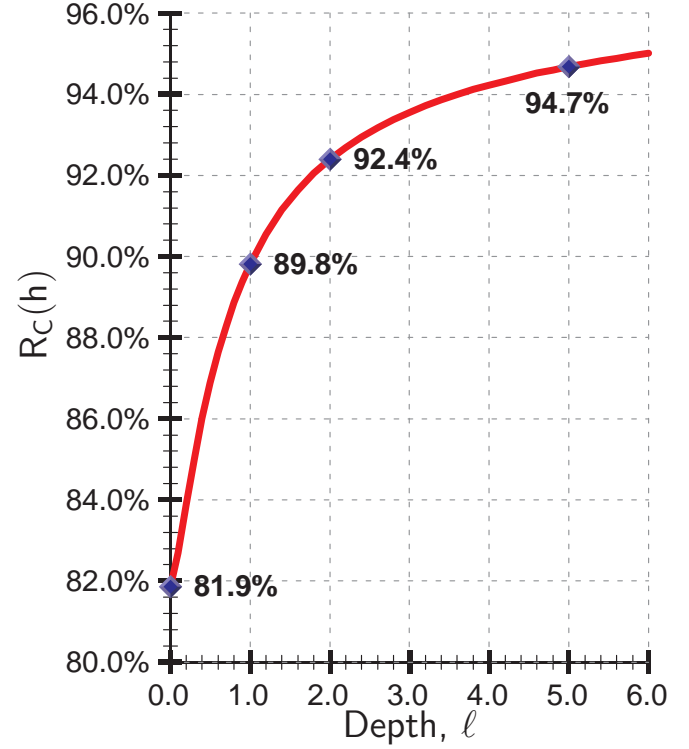


FIG. 9: Ratio $R_C(h)$ between the integral coherent intensity given by the diffusion approximation and full integral coherent intensity for various depths, where the integration is taken over $1/k\ell$.

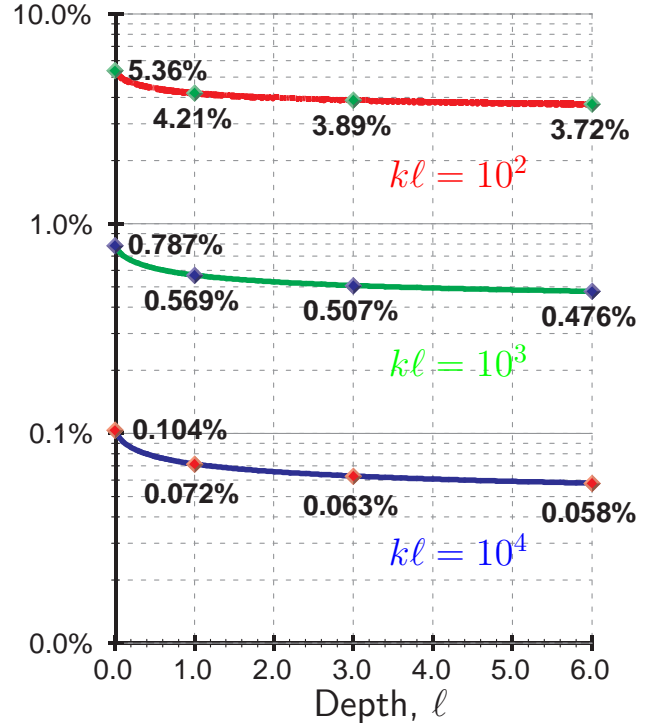


FIG. 10: Ratio between the integral coherent intensity and integral incoherent intensity for various depths and various $k\ell$.

the maximally-crossed diagrams.

Finally on Fig. 9 is represented the ratio, multiplied by $k\ell$, between the integral magnitudes of the coherent and incoherent scattered intensity. It is naturally, that the integral coherent intensity is proportional to the perturbation theory parameter $1/k\ell$, moreover this proportionality becomes linear for sufficiently small $1/k\ell$. But the ratio, shown on Fig. ??, also depends on $k\ell$, so the above mentioned relationship is not fulfilled in the diffusion approximation. An important conclusion, we can derive from Fig. 9, is that the coherent scattering is an effective surface phenomenon.

X. CONCLUSION.

The main result of the present paper are the exact expressions for the incoherent (60) and coherent (71) intensity of a scalar wave scattered by semi-infinite disordered media in the general case of moving scatterers. The intensities are found as functions of the observation point and wave vector direction for all values of the solid angle (4π - geometry). This allows us to analyze critically all the approximations done previously and to evaluate their deviation from the exact result.

In the case of multiple scattering in disordered media the far most popular approximation is the diffusion approximation. However although in some papers^{11,16,19} it was mentioned that the diffusion approximation does not give correct results even for the simplest case of incoherent intensity, which corresponds to the summation of all ladder graphs in the mass operator, it does not exist analysis of the deviation of the exact results from these obtained in the diffusion approximation. We performed this kind of analysis in several important cases.

For the simplest case of statistical homogeneous and isotropic medium of static point-like ideal scatterers we found that the systematic error due to the diffusion approximation for the incoherent intensity on the surface and for various directions is about 6-7%. We obtained that the error decreases in depth of the half space and at infinity becomes zero.

For the case of coherent scattering it is well known that the diffusion approximation gives acceptable results for small angles around π inside the region $\pi+1/k\ell$. In this paper we demonstrated quantitatively the deviation from the exact result. Even in backward direction on the surface of the medium the diffusion approximation does not reproduce the exact result but gives the same error (7%) as in the incoherent case. Away from the backward direction the relative contribution of the diffusion approximation term of the coherent intensity dramatically decreases. Our expression (71) gives the possibility to calculate the coherent intensity for any value of the scattering angle including in forward direction. For this particular case the diffusion approximation is an order of magnitude smaller than the exact result.

In the case when the multiple coherent backscattering

is also taken into account the diffusion approximation for the intensity breaks down for large deviations from backward direction. The usual explanation of this fact is the incorrect description in this case of the interference effects for scattering with low multiplicity order^{11,16}. In order to check this conjecture we had to obtain explicit and exact expressions for the intensities with fixed multiplicity order ("partial" intensities). A natural starting point to do this are the derived in Chapters V and VI exact expressions for the incoherent and coherent part of the intensities. Then the problem is reduced to correct and consistent transition from the diffusion approximation of the exact propagator to the diffusion approximation of the propagators with given order of multiplicity of the scattering. The consistency is the fulfillment of the condition that with increasing the number of the partial intensities which we sum up the sum should converge to the total intensity scattered at given angle. Until present work the only known results in this direction were the obtained in the expressions for the partial coherent intensities in the case of static point scatterers. However they did not fulfil the above formulated consistency condition. The key to the solution of this problem is the understanding that **the diffusion approximation considered as asymptotic case for $R \gg \ell^{25}$ do not match with the spread opinion that it corresponds to an approximation for the Fourier transform $\tilde{L}(K, t)$, where for $K \ll 1/\ell$ $\arctg K\ell/K\ell \approx 1 - (K\ell)^2/3$** . It is clear that the cut off in the variable K is not a correct procedure, when representing $\tilde{L}(R, t)$ with its Fourier transform $\tilde{L}(K, t)$. This leads to the wrong guess for the geometrical series base for $\tilde{L}(K, t)$ and therefore to wrong results for the partial intensities for a given scattering angle in diffusion approximation¹⁶. The proposed by us procedure for the diffusion approximation of the partial intensities is consistent. For example the sum of the first 30 multiplicity orders for the multiple coherent backscattering intensity give 60.1602% for angle $\pi - \alpha := 0$ and 99.9972% for angle $\pi - \alpha := \lambda/2\pi\ell$.

The comparison of the coherent intensities for 2, 3, 4, 5, 6 and 7 multiplicity orders of scattering calculated with the exact formula and our formula in diffusion approximation demonstrates an increase of the relative deviation $(J_n^C - {}^d J_n^C)/J_n^C$ with increasing the angle $\pi - \alpha$. For a fixed value of the angle the relative deviation increases with increasing of the multiplicity order. In the same time because of the sharp decrease of the contribution of a given multiplicity order the deviation $(J_n^C - {}^d J_n^C)/J^C$ is largest in case of double scattering. Only in this sense one may say that the low multiplicity orders of scattering are cut for large values of $\pi - \alpha$.

When we investigated the behaviour of the integral incoherent intensity, we found the same degree of validity of diffusion approximation as the differential intensity. But it is more interesting for us, what is happened with the integral coherent intensity. If the polar angle scale, for which the diffusion approximation is acceptable, is limited to $1/k\ell$, the corresponding solid angle scale is

$\leq \pi/k^2\ell^2$. That's why the diffusion approximation gives a **drastic deviation from the correct values of the integral coherent intensity** (Fig. 103), compared to the deviation of the differential coherent intensity for a fixed large angle. It is noteworthy that the integral coherent intensity, calculated by the exact expression, depends linearly on the perturbation parameter $1/k\ell$ for $k\ell \gg 1$. This dependence is not satisfied in the diffusion approximation. When we set ourselves the problem for the energy losses due to coherent scattering, we should have in mind that, **the main integral intensity originates from the scattering directions far from the backscattering peak**. That's why if someone is interesting in such item he will have to integrate the exact expression (71) in 4π -geometry.

We have to remark, that the represented results for scattering intensity are obtained for Miln boundary problem, solved in diffusion approximation²⁵, where the Miln number is 0,7104. However the exact value of the Miln number is a bit different, but in our opinion it could not essentially influence on the represented numerical results.

The way of obtaining the exact results for the case of half-space, allows an extension of the method to the case of flat or spherical slab. In the standard approach the authors^{11,16,19} found the explicit form of the coherent propagator in space variables as a Fourier transform of the time-reversed ladder propagator in wave-vector representation. After that they replaced it in the coherent intensity expression. In this work we perform a second

operation of time-reversal directly inside the coherent intensity expression. The last is expressed by the ladder propagator in space variables, which have the same sequence like this one in the incoherent intensity expression and the Green function variables have the exchanged places.

Our formulas conserve their validity also for small effective diffusion length. That means, they can describe the case of fast nonrelativistic scatterer motions as well as strong absorption. These situations lead to a cut off the constructive interference for higher order scattering and suppressing of the coherent effects.

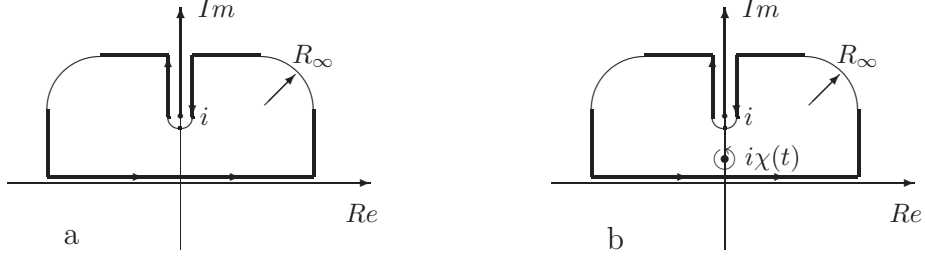
If somebody keep his attention and interest in the content of this paper, he could have a background for an improvement of the popular results for the multiple scattering of the polarized light or to think about how it could be taken into account the scatterer size in further investigations.

XI. ACKNOWLEDGMENTS

The author would like to thank Prof. Matey Mateev, who introduced me to the problem and helped me with encouragement and numerous fruitful discussions. Also I am grateful to Drs M. Kostov and J. Velev for scientific and technical support and to Ch. Palamarev, who help me with software.

-
- ¹ P.W. Anderson, Phys.Rev., **109**, 1492 (1958)
² N.F. Mott, Adv. Phys., **16**, 49 (1967)
³ N.F. Mott, Phyl. Mag., **22**, 7 (1970)
⁴ F. Wegner, Zeit. Phys., **B35**, 207 (1979)
⁵ D. Vollhardt and P. Wölfle, Phys. Rev., **B22**, 4666 (1980)
⁶ E. Abrahams, P.W. Anderson, D.C. Lucciardello and T.V. Ramakrishnan, Phys. Rev. Lett., **42**, 673 (1979)
⁷ P. Lee and T.V. Ramakrishnan, Rev. Mod. Phys., **57**, 287 (1985)
⁸ Yu. N. Barabanenkov, Izv. Vyssh. Uchebn. Zaved., **XVI**, 88 (1973)
⁹ S. John et al., Phys. Rev., **B27**, 5592 (1983)
¹⁰ S. John, Phys. Rev. Lett., **53**, 2169 (1984)
¹¹ A.A. Golubentsev, Zh. Eksp. Teor. Fiz. **86**, 47 (1984) [Sov. Phys.-JETP **59**, 26 (1984)].
¹² P.W. Anderson, Phyl. Mag., **B52**,505 (1985)
¹³ L. Tzang, A. Ishimaru, J.Opt.Soc.Am **A2**, 1331 (1985).
¹⁴ M. J. Stephen, Phys. Rev. Lett. **56**, 1809 (1986).
¹⁵ M. J. Stephen and G. Cwilich, Phys. Rev. B **34**, 7564 (1986).
¹⁶ E. Akkermans, P.E. Wolf, R. Maynard & G. Maret, J. Phys. France **49**, 77 (1988).
¹⁷ M. J. Stephen, Phys. Rev. B **37**, 1 (1988).
¹⁸ M. J. Stephen, *Mesoscopic Phenomena in Solids* – Chapter 3, Elsevier Science Publishers B.V.,1991.
¹⁹ Mac Kintosh & Sajeev John, Phys. Rev. B, **37**, 1884 (1988).
²⁰ Mac Kintosh & Sajeev John, Phys. Rev. B, **40**, 2383 (1989).
²¹ Ping Sheng ed. 1990, Scattering and localization of Classical Waves in Random Media, World Scientific (1990)
²² M.P. van Albada and A. Lagendijk, Phys. Rev. Lett. **55**, 2692 (1985).
²³ P.E. Wolf and G.Maret, Phys. Rev. Lett. **55**, 2696 (1985).
²⁴ M. Kaveh, M. Rosenbluh, I. Edrei and I. Freund, Phys. Rev. Lett. **57**, 2049 (1986).
²⁵ B. Devison & J.B. Sykes, *Neutron Transport Theory* (Oxford University, New York, 1957).
²⁶ S.M. Ritov, Y.A. Kwartzov, V.I. Tatarskii *Introduction in Statistical Radiophysics* Moscow "Nauka" (in Russian).
²⁷ A.Ishimaru, *Wave Propagation and Scattering in Random Media* (Academic Press, New York, London, San Francisco, 1978).
²⁸ M.V. van der Mark and M.P. van Albada, A. Lagendijk, Phys. Rev. B, **37**, 3575 (1988).
²⁹ M.B. Hastings, A.D. Stone, H.u. Baranger, Phys. Rev. B **50**, 8230 (1994).
³⁰ D.D.Clayton *Principles of Stellar Evolution and Nucleosynthesis*, The University of Chicago Press edition 1983.
³¹ G. Placzek and W. Seidel, Phys. Rev. **72**, 550 (1947).
³² C. Mark, Phys. Rev. **72**, 558 (1947).
³³ J.S. Langer and T. Neal, Phys. Rev. Lett. **16**, 984 (1966).

1. Calculation of the L_n in space variables.



$$\begin{aligned}
\int_{-\infty}^{+\infty} e^{i\frac{R}{\ell}p} \left(\frac{\text{arctg} p}{p} \right)^n p dp &= \lim_{\epsilon \rightarrow 0+} \left\{ \lim_{|z| \rightarrow \infty} \int_{\pi}^{\arccos \frac{\epsilon}{|z|}} e^{i\frac{R}{\ell}|z|e^{i\varphi}} \frac{\text{arctg}(|z|e^{i\varphi})}{|z|e^{i\varphi}} |z|^2 i e^{2i\varphi} d\varphi + \right. \\
&+ \int_{+i\infty-\epsilon}^{i-\epsilon} e^{i\frac{R}{\ell}z} \left(\frac{\text{arctg} z}{z} \right)^n z dz + i \epsilon \int_{-\pi}^0 e^{-\frac{R}{\ell}(1-i\epsilon e^{i\varphi})} \left[\frac{\text{arctg}(i + \epsilon e^{i\varphi})}{i + \epsilon e^{i\varphi}} \right]^n (i + \epsilon e^{i\varphi}) e^{i\varphi} d\varphi + \\
&\left. + \int_{i+\epsilon}^{i\infty+\epsilon} e^{i\frac{R}{\ell}z} \left(\frac{\text{arctg} z}{z} \right)^n z dz + \lim_{|z| \rightarrow \infty} \int_0^{\arccos \frac{\epsilon}{|z|}} e^{i\frac{R}{\ell}|z|e^{i\varphi}} \frac{\text{arctg}(|z|e^{i\varphi})}{|z|e^{i\varphi}} |z|^2 i e^{2i\varphi} d\varphi \right\} \quad (96)
\end{aligned}$$

Only second and fourth terms give nonzero yield in the integral (96), so

$$\begin{aligned}
\int_{-\infty}^{+\infty} e^{i\frac{R}{\ell}p} \left(\frac{\text{arctg} p}{p} \right)^n p dp &= \lim_{\delta \rightarrow 0+} i \int_{1+\delta}^{\infty} \lim_{\epsilon \rightarrow 0+} \left\{ \frac{e^{-\frac{R}{\ell}(u-i\epsilon)}}{(iu + \epsilon)^{n-1}} [\text{arctg}(iu + \epsilon)]^n - \frac{e^{-\frac{R}{\ell}(u+i\epsilon)}}{(iu - \epsilon)^{n-1}} [\text{arctg}(iu - \epsilon)]^n \right\} du = \\
&= \int_1^{\infty} \frac{e^{-\frac{R}{\ell}u}}{2^n u^{n-1}} \left[\left(\ln \frac{u+1}{u-1} + i\pi \right)^n - \left(\ln \frac{u+1}{u-1} - i\pi \right)^n \right] du = i \int_1^{\infty} \frac{e^{-\frac{R}{\ell}u}}{(2u)^{n-1}} \left(\ln^2 \frac{u+1}{u-1} + \pi^2 \right)^{\frac{n}{2}} \sin \left(n \arctg \frac{\pi}{\ln \frac{u+1}{u-1}} \right) du
\end{aligned}$$

Replacing this result in (34) we will have the following expressions for first 6 bare ladder diagrams:

$$\begin{aligned}
L_2(R, t) &= \frac{g^2(t)}{R \ell^3} \int_1^{\infty} \exp\left(-R \frac{u}{\ell}\right) du = \frac{g^2(t) \exp\left(-\frac{R}{\ell}\right)}{R^2 \ell^2} \\
L_3(R, t) &= \frac{g^3(t)}{R \ell^3} \int_1^{\infty} \frac{\exp\left(-R \frac{u}{\ell}\right)}{u} \ln \frac{u+1}{u-1} du \\
L_4(R, t) &= \frac{g^4(t)}{R \ell^3} \int_1^{\infty} \frac{\exp\left(-R \frac{u}{\ell}\right)}{(2u)^2} \left(3 \ln^2 \frac{u+1}{u-1} - \pi^2 \right) du \\
L_5(R, t) &= \frac{g^5(t)}{R \ell^3} \int_1^{\infty} \frac{\exp\left(-R \frac{u}{\ell}\right)}{2u^3} \ln \frac{u+1}{u-1} \left(\ln^2 \frac{u+1}{u-1} - \pi^2 \right) du \\
L_6(R, t) &= \frac{g^6(t)}{R \ell^3} \int_1^{\infty} \frac{\exp\left(-R \frac{u}{\ell}\right)}{16u^4} \left(5 \ln^4 \frac{u+1}{u-1} - 10\pi^2 \ln^2 \frac{u+1}{u-1} + \pi^4 \right) du \\
L_7(R, t) &= \frac{g^7(t)}{R \ell^3} \int_1^{\infty} \frac{\exp\left(-R \frac{u}{\ell}\right)}{16u^5} \ln \frac{u+1}{u-1} \left(3 \ln^4 \frac{u+1}{u-1} - 10\pi^2 \ln^2 \frac{u+1}{u-1} + 3\pi^4 \right) du
\end{aligned} \quad (97)$$

2. Calculation of the \tilde{L} in space variables.

$$\begin{aligned}
\int_{-\infty}^{+\infty} \frac{\operatorname{arctg} p e^{ip \frac{R}{t}} dp}{g^{-1}(t) - \frac{\operatorname{arctg} p}{p}} &= 2\pi i \operatorname{Res}_{|z=iX} \frac{\operatorname{arctg} z \exp(-iz \frac{R}{t})}{g^{-1}(t) - \frac{\operatorname{arctg}(z)}{z}} + \\
&+ \lim_{\epsilon \rightarrow 0^+} \left\{ i \int_1^{\infty} \left[\frac{e^{(-u+i\epsilon) \frac{R}{t}} \operatorname{arctg}(iu+\epsilon)}{g^{-1}(t) - \frac{\operatorname{arctg}(iu+\epsilon)}{iu+\epsilon}} - \frac{e^{(-u-i\epsilon) \frac{R}{t}} \operatorname{arctg}(iu-\epsilon)}{g^{-1}(t) - \frac{\operatorname{arctg}(iu-\epsilon)}{iu-\epsilon}} \right] du + \int_{-\pi}^0 \frac{\operatorname{arctg}(i + \epsilon e^{i\varphi}) e^{-\frac{R}{t}(1+\epsilon \sin \varphi)} e^{i \frac{R}{t} \epsilon \cos \varphi} i \epsilon e^{i\varphi}}{g^{-1}(t) - \frac{\operatorname{arctg}(i + \epsilon e^{i\varphi})}{i + \epsilon e^{i\varphi}}} d\varphi - \right. \\
&\left. - \lim_{|z| \rightarrow \infty} |z| \left[\int_0^{\arccos \frac{\epsilon}{|z|}} \frac{\operatorname{arctg}(|z| e^{i\varphi}) e^{-\frac{R}{t}|z| \sin \varphi} e^{i \frac{R}{t}|z| \cos \varphi} i e^{i\varphi}}{g^{-1}(t) - \frac{\operatorname{arctg}(|z| e^{i\varphi})}{|z| e^{i\varphi}}} d\varphi + \int_{-\arccos \frac{\epsilon}{|z|}}^0 \frac{\operatorname{arctg}(|z| e^{i\varphi}) e^{\frac{R}{t}|z| \sin \varphi} e^{-i \frac{R}{t}|z| \cos \varphi} i e^{i\varphi}}{g^{-1}(t) - \frac{\operatorname{arctg}(|z| e^{i\varphi})}{|z| e^{i\varphi}}} d\varphi \right] \right\} \quad (98)
\end{aligned}$$

3. 3D δ -function.

$$\begin{aligned}
\delta(k\vec{S} - k_0\vec{S}_{RR_1}) &= \quad (99) \\
&= \delta \left(k \sin \alpha + k_0 \frac{X_1}{\sqrt{X_1^2 + Y_1^2 + (Z-Z_1)^2}} \right) \delta \left(k_0 \frac{Y_1}{\sqrt{X_1^2 + Y_1^2 + (Z-Z_1)^2}} \right) \delta \left(k \cos \alpha - k_0 \frac{Z-Z_1}{\sqrt{X_1^2 + Y_1^2 + (Z-Z_1)^2}} \right) = \\
&= \frac{\sqrt{X_1^2 + (Z-Z_1)^2}}{k_0} \delta \left(k \sin \alpha + \frac{k_0 X_1}{\sqrt{X_1^2 + (Z-Z_1)^2}} \right) \delta(Y_1) \delta \left(k \cos \alpha - \frac{k_0(Z-Z_1)}{\sqrt{X_1^2 + (Z-Z_1)^2}} \right) = \\
&= \frac{(Z-Z_1)^2}{k_0^2 \cos^4 \alpha} \left| \cos \alpha + \frac{\sin^2 \alpha}{|\cos \alpha|} \frac{Z-Z_1}{|Z-Z_1|} \right|^{-1} \theta \left(\frac{Z-Z_1}{\cos \alpha} \right) \delta(k - k_0) \delta \left(X_1 + \sin \alpha \frac{|Z-Z_1|}{|\cos \alpha|} \right) \delta(Y_1) = \\
&= \begin{cases} \frac{Z-Z_1}{k_0^2 |\cos \alpha|^3} \delta(k - k_0) \delta(X_1 + \operatorname{tg} \alpha (Z-Z_1)) \delta(Y_1) \theta \left(\frac{Z-Z_1}{\cos \alpha} \right) & ; \alpha \neq \pi/2 \\ \frac{X_1^2}{k_0^2} \delta \left(k + k_0 \frac{X_1}{|X_1|} \right) \delta(Y_1) \delta(Z-Z_1) = \frac{X_1^2}{k_0^2} \delta(k - k_0) \delta(Y_1) \delta(Z-Z_1) \Theta(-X_1) & ; \alpha = \pi/2 \end{cases}
\end{aligned}$$

4. Calculation of single scattering intensity.

$$L_1(\vec{R}_1, \vec{R}_2; k_0\vec{S}_1, k_0\vec{S}_2; t) = \delta(\vec{R}_1 - \vec{R}_2) \Phi(k_0(\vec{S}_1 - \vec{S}_2), t) \approx \frac{4\pi}{\ell} \delta(\vec{R}_1 - \vec{R}_2) g(t) \quad (100)$$

$$\Gamma_1(\vec{R}, \vec{k}; t) := \int \exp(-i\vec{k} \cdot \vec{r}) \Gamma_{L_1}(\vec{R}, \vec{r}; t) d^3\vec{r} = \frac{2\pi^2}{\ell} g(t) e^{-i\omega_0 t} \int \delta(\vec{k} - k_0\vec{S}_{RR_1}) \frac{\exp \frac{-|\vec{R}-\vec{R}_1|}{\ell}}{(\vec{R}-\vec{R}_1)^2} |E(\vec{R}_1)|^2 d^3\vec{R}_1 \quad (101)$$

$$J_1(Z, \alpha, t) = \frac{g(t)\pi^2 |E_0|^2 e^{-i\omega_0 t}}{2\ell |\cos \alpha|} \int_0^{+\infty} \theta \left(\frac{Z-Z_1}{\cos \alpha} \right) \exp \left(\frac{Z_1-Z}{\ell \cos \alpha} \right) e^{-\frac{Z_1}{\ell}} dZ_1 \quad (102)$$

$$J_1(h, \alpha, t) = 2\pi^2 |E_0|^2 e^{-i\omega_0 t} g(t) \frac{e^{-h} - \theta(\cos \alpha) e^{-\frac{h}{\cos \alpha}}}{1 - \cos \alpha} \quad (103)$$

5. Albedo

$$H^C(0, \alpha, u) = \frac{1}{(1 - (1+\xi)\cos \alpha)^2 + (\eta \cos \alpha)^2} \left(\frac{\cos \alpha}{\cos \alpha - 1} + \frac{1 - e^{-M\xi}}{\xi} \right); \quad \frac{\pi}{2} \leq \alpha \leq \pi \quad (104)$$

6. Calculation of partial intensities.

$$\begin{aligned}
J_{n+1}^{L\text{diff}}(h, 0, t) = & 2\pi^2 |E_0|^2 e^{-i\omega_0 t} g(t) \left\{ \left(\frac{3 + \chi_1^2(t)}{2 + \chi_1^2(t)} \right)^n h e^{-h} + \right. & u := \sqrt{3 + 2\chi_1^2(t)} \\
& + (3 + \chi_1^2(t))^n \sum_{k=1}^n \binom{2n-k-1}{n-1} (2u)^{k-2n} \sum_{m=0}^{k-1} \frac{1}{m!} [(k-m)(u-1)^{m-k-1} (h^m e^{-uh} - \theta(-m)e^{-h}) - \\
& \left. - \frac{(u+1)^{m-k} - (u-1)^{m-k}}{2} ((h+2M_{as})^m \exp(-u(h+2M_{as})) - (2M_{as})^m \exp(-2uM_{as}-h)) \right] \Big\} \quad (105)
\end{aligned}$$

$$\begin{aligned}
J_{n+1}^{L\text{diff}}\left(h, \frac{\pi}{2}, t\right) = & 2\pi^2 |E_0|^2 e^{-i\omega_0 t} g(t) \left\{ \left(\frac{3 + \chi_1^2(t)}{2 + \chi_1^2(t)} \right)^n e^{-h} + \right. & (106) \\
& \left. + (3 + \chi_1^2(t))^n \sum_{k=1}^n \binom{2n-k-1}{n-1} (2u)^{k-2n} \sum_{m=0}^{k-1} \frac{1}{m!} [h^m e^{-uh} (u-1)^{m-k} + (h+2M_{as})^m \exp(-u(h+2M_{as})) (u+1)^{m-k}] \right\}
\end{aligned}$$

$$\begin{aligned}
J_{n+1}^{L\text{diff}}(h, \pi, t) = & 2\pi^2 |E_0|^2 e^{-i\omega_0 t} g(t) \left\{ \left(\frac{3 + \chi_1^2(t)}{2 + \chi_1^2(t)} \right)^n \frac{e^{-h}}{2} + (3 + \chi_1^2(t))^n \sum_{k=1}^n \binom{2n-k-1}{n-1} (2u)^{k-2n} \times \right. & (107) \\
& \left. \times \sum_{m=0}^{k-1} \frac{1}{m!} \left[h^m e^{-uh} \frac{(u+1)^{m-k} - (u-1)^{m-k}}{2} - (h+2M_{as})^m \exp(-u(h+2M_{as})) (k-m)(u+1)^{m-k-1} \right] \right\}
\end{aligned}$$